Gastroenterology 2019;157:1615–1629

BASIC AND TRANSLATIONAL—LIVER

New High-Throughput Screening Identifies Compounds That Reduce Viability Specifically in Liver Cancer Cells That Express High Levels of SALL4 by Inhibiting Oxidative Phosphorylation

Justin L. Tan,[1,2,*,§] **Feng Li**,[1,*] Joanna Z. Yeo,[1,2] Kol Jia Yong,[1] Mahmoud A. Bassal,[1,3] Guo Hao Ng,[2] May Yin Lee,[2] Chung Yan Leong,[4] Hong Kee Tan,[1] Chan-shuo Wu,[1] Bee Hui Liu,[1] Tim H. Chan,[1] Zi Hui Tan,[1] Yun Shen Chan,[2] Siyu Wang,[2] Zhi Han Lim,[2] Tan Boon Toh,[1] Lissa Hooi,[1] Kia Ngee Low,[4] Siming Ma,[2] Nikki R. Kong,[5] Alicia J. Stein,[5] Yue Wu,[5,6] Matan T. Thangavelu,[2] Atsushi Suzuki,[7] Giridharan Periyasamy,[2] John M. Asara,[8] Yock Young Dan,[1,9,10] Glenn K. Bonney,[11,12] Edward K. Chow,[1,13] Guo-Dong Lu,[1,14,15] Huck Hui Ng,[2] Yoganathan Kanagasundaram,[4] Siew Bee Ng,[4] Wai Leong Tam,[1,2,16,17,§] Daniel G. Tenen,[1,3,§] and Li Chai[5,§]

*[1]Cancer Science Institute of Singapore, National University of Singapore, Singapore; [2]Genome Institute of Singapore, Agency for Science, Technology and Research (A*STAR), Singapore; [3]Harvard Stem Cell Institute, Harvard Medical School, Boston, Massachusetts; [4]Bioinformatics Institute, Agency for Science, Technology and Research (A*STAR), Singapore; [5]Department of Pathology, Brigham & Women's Hospital, Harvard Medical School, Boston, Massachusetts; [6]Department of Clinical Laboratory, National Cancer Center/Cancer Hospital, Chinese Academy of Medical Sciences and Peking Union Medical College, Beijing, China; [7]Division of Organogenesis and Regeneration, Medical Institute of Bioregulation, Kyushu University, Fukuoka, Japan; [8]Department of Medicine, Division of Signal Transduction, Beth Israel Deaconess Medical Center and Harvard Medical School, Boston, Massachusetts; [9]Department of Medicine, Yong Loo Lin School of Medicine, National University of Singapore, Singapore; [10]Division of Gastroenterology and Hepatology, University Medicine Cluster, National University Health System, Singapore; [11]Department of Hepatobiliary, Pancreatic Surgery and Liver Transplantation, Department of Surgery, University Surgical Cluster, National University Health System, Singapore; [12]National University Centre for Organ Transplantation, National University Hospital, Singapore; [13]Department of Pharmacology, Yong Loo Lin School of Medicine, National University of Singapore, Singapore; [14]Department of Toxicology, School of Public Health, Guangxi Medical University, Nanning, China; [15]Key Laboratory of High-Incidence-Tumor Prevention and Treatment (Guangxi Medical University), Ministry of Education of China, Nanning, China; [16]Department of Biochemistry, Yong Loo Lin School of Medicine, National University of Singapore, Singapore; and [17]School of Biological Sciences, Nanyang Technological University, Singapore*

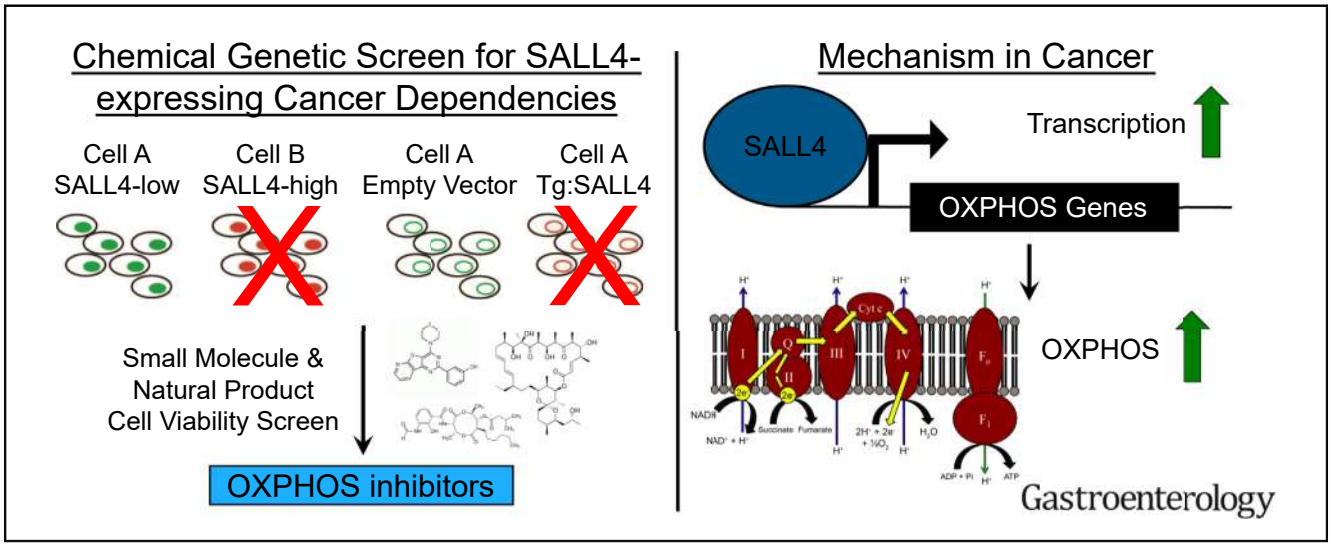

See editorial on page 1475.

BACKGROUND & AIMS: Some oncogenes encode transcription factors, but few drugs have been successfully developed to block their activity specifically in cancer cells. The transcription factor SALL4 is aberrantly expressed in solid tumor and leukemia cells. We developed a screen to identify compounds that reduce the viability of liver cancer cells that express high levels of SALL4, and we investigated their mechanisms. **METHODS:** We developed a stringent high-throughput screening platform comprising unmodified SNU-387 and SNU-398 liver cancer cell

lines and SNU-387 cell lines engineered to express low and high levels of SALL4. We screened 1597 pharmacologically active small molecules and 21,575 natural product extracts from plant, bacteria, and fungal sources for those that selectively reduce the viability of cells with high levels of SALL4 (SALL4^{hi} cells). We compared gene expression patterns of SALL4^{hi} cells vs SALL4-knockdown cells using RNA sequencing and real-time polymerase chain reaction analyses. Xenograft tumors were grown in NOD/SCID gamma mice from SALL4^{hi} SNU-398 or HCC26.1 cells or from SALL4^{lo} patient-derived xenograft (PDX) cells; mice were given injections of identified compounds or sorafenib, and the effects on tumor growth were measured. **RESULTS:** Our screening identified 1 small molecule (PI-103) and 4 natural compound analogues (oligomycin, efrapeptin, antimycin, and leucinostatin) that selectively reduced viability of SALL4^{hi} cells. We performed validation studies, and 4 of these compounds were found to inhibit oxidative phosphorylation. The adenosine triphosphate (ATP) synthase inhibitor oligomycin reduced the viability of SALL4^{hi} hepatocellular carcinoma and non–small-cell lung cancer cell lines with minimal effects on SALL4^{lo} cells. Oligomycin also reduced the growth of xenograft tumors grown from SALL4^{hi} SNU-398 or HCC26.1 cells to a greater extent than sorafenib, but oligomycin had little effect on tumors grown from SALL4^{lo} PDX cells. Oligomycin was not toxic to mice. Analyses of chromatin immunoprecipitation sequencing data showed that SALL4 binds approximately 50% of mitochondrial genes, including many oxidative phosphorylation genes, to activate their transcription. In comparing SALL4^{hi} and SALL4-knockdown cells, we found SALL4 to increase oxidative phosphorylation, oxygen consumption rate, mitochondrial membrane potential, and use of oxidative phosphorylation–related metabolites to generate ATP. **CONCLUSIONS:** In a screening for compounds that reduce the viability of cells that express high levels of the transcription factor SALL4, we identified inhibitors of oxidative phosphorylation, which slowed the growth of xenograft tumors from SALL4^{hi} cells in mice. SALL4 activates the transcription of genes that regulate oxidative phosphorylation to increase oxygen consumption, mitochondrial membrane potential, and ATP generation in cancer cells. Inhibitors of oxidative phosphorylation might be used for the treatment of liver tumors with high levels of SALL4.

Keywords: Chemical-Genetic Screen; HCC; Metabolic Vulnerability; Metabolism.

WHAT YOU NEED TO KNOW

BACKGROUND AND CONTEXT

The transcription factor SALL4 is mis-expressed in cancer cells. We developed a screen to identify compounds that reduce the viability of liver cancer cells that mis-express SALL4 and the mechanisms by which these compounds act.

NEW FINDINGS

We identified a metabolic vulnerability in liver (and possibly lung) cancer cells, due to overexpression of SALL4, which can be targeted by natural product oxidative phosphorylation inhibitors.

LIMITATIONS

This was a chemical screen for compounds that affect the viability of a small number of cell lines in culture and growth as xenograft tumors in mice. Additional studies in other animal models of liver cancer, and on other cell lines, are needed.

IMPACT

We developed a screen to identify compounds that kill cancer cells that overexpress or underexpress a specific protein. This screen can be used to identify compounds with toxicity to cells with other alterations in gene expression and identify the mechanisms regulated by these alterations.

Transcription factors are the second largest class of oncogenes.[1] However, the molecular mechanisms by which these transcription factors exert their cancer-driving effects are not well understood. There is renewed interest in phenotypic cell-based screenings for studying the underlying mechanisms of various diseases, aiding in subsequent drug discovery.[2] Common methods for cell-based drug discovery include the screening of endogenous cell lines with and without the gene or mutation of interest or the use of isogenic cell line systems in which the gene of interest is altered or expressed in an unaffected cell to control for genetic background.[2,3] In both endogenous and isogenic systems, hits are defined by their ability to selectively target cells expressing the alteration of interest while not affecting the control cells. The disadvantage of the endogenous system is that cell lines are genetically distinct, so hits obtained may target pathways unrelated to the alteration of interest.[2] The isogenic system avoids the genetic complexity of the endogenous system but has the drawback of compound interference with the transgene, resulting in hits that might not be biologically relevant.[4] To overcome these drawbacks, we developed a screening platform that encompasses both endogenous and isogenic methodologies, applying the platform to identify vulnerabilities induced by oncogene SALL4 misexpression in hepatocellular carcinoma (HCC).

Liver cancer is the sixth most common cancer, but it is the second leading cause of cancer deaths worldwide because of limited therapeutic interventions.[5] HCC is the predominant subtype of liver cancer, with 85% of patients with liver cancer having HCC. The only approved targeted therapies for treating HCC, kinase inhibitors sorafenib and

* Authors share co-first authorship; § Authors share co-senior authorship.

Abbreviations used in this paper: ATP, adenosine triphosphate; ChIP-seq, chromatin immunoprecipitation sequencing; GEO, Gene Expression Omnibus; HCC, hepatocellular carcinoma; IC_{50}, median inhibitory concentration; mRNA, messenger RNA; mtDNA, mitochondrial DNA; mTOR, mammalian target of rapamycin; NADH, reduced nicotinamide adenine dinucleotide; NSCLC, non–small-cell lung cancer; NuRD, nucleosome remodeling and deacetylase complex; OCR, oxygen consumption rate; PDX, patient-derived xenograft; PI3K, phosphoinositide 3-kinase; RNA-seq, RNA sequencing; SALL4, Spalt-like transcription factor 4.

Most current article

0016-5085/$36.00
https://doi.org/10.1053/j.gastro.2019.08.022

regorafenib, target tumor vasculature, but they are largely ineffective and are used as a last resort.[6,7] There is an increased urgency to discover precision medicine interventions for this unmet need.

SALL4 (Spalt-like transcription factor 4) is an oncofetal protein essential for self-renewal and for maintaining pluripotency in embryonic stem cells, and it plays a critical role in early embryonic development.[8–11] It is subsequently silenced in most adult tissues but is aberrantly re-expressed to drive tumorigenesis in various cancers.[9,12] *SALL4* is highly expressed in fetal liver but is silenced in the adult liver,[13] and it is often reactivated in HCC, in which 30%–50% of tumors show significant *SALL4* expression.[14] There are 2 isoforms of *SALL4* (*SALL4A* and *SALL4B*) that have overlapping but nonidentical binding regions in the genome, and *SALL4B* alone can maintain pluripotency.[15] Both isoforms are derived from the same transcript, where SALL4A is the full-length spliceoform and SALL4B lacks part of exon 2.[9,16] It has been observed that both *SALL4* isoforms are coexpressed when *SALL4* is transcriptionally up-regulated.[14] *SALL4* is a C2H2 zinc-finger transcription factor that can act as a transcriptional activator or repressor.[15,17,18] The repressive function of SALL4 is achieved through recruitment of the nucleosome remodeling and deacetylase complex (NuRD).[19] In cancer, SALL4 recruits NuRD to genes such as the *PTEN* tumor suppressor, deacetylating and silencing the locus.[19] The transcriptional activation function of SALL4 also plays a role in cancer. SALL4 has been shown to transcriptionally activate the c-MYC oncogene in endometrial cancer[20] and HOXA9 in acute myeloid leukemia.[21] The in vivo tumorigenic potential of SALL4 is reflected in a mouse model of constitutive *SALL4B* expression, which results in the onset of acute myeloid leukemia and HCC.[22] Therapeutic interventions that target SALL4 and its dependencies remain elusive.

Here, we developed a screening platform that encompasses both endogenous and isogenic methodologies, applying the platform to discover drugs targeting oncogene SALL4-induced dependencies in HCC. Our platform uses an endogenous pair of SALL4-expressing ($SALL4^{hi}$) and SALL4-undetectable ($SALL4^{lo}$) HCC cell lines, as well as isogenic SALL4-undetectable cell lines engineered to express SALL4 isoforms. We screened both synthetic and diverse natural product extract libraries to identify hit compounds that specifically decrease $SALL4^{hi}$ cell viability. Unexpectedly, our screening identified 4 oxidative phosphorylation inhibitors as being selective for $SALL4^{hi}$ cells. Our most potent and selective compound, the adenosine triphosphate (ATP) synthase inhibitor oligomycin, can selectively target a panel of $SALL4^{hi}$ HCC and lung cancer cell lines over $SALL4^{lo}$ cells. Oligomycin also shows in vivo tumor suppressive activity similar to that of the HCC standard-of-care drug sorafenib, but at a dose 200 times lower. This in vivo efficacy is observed only in $SALL4^{hi}$ and not $SALL4^{lo}$ tumors. Analysis of SALL4 chromatin immunoprecipitation sequencing (ChIP-seq) data showed SALL4 binding to a significant number of oxidative phosphorylation genes in $SALL4^{hi}$ HCC. SALL4 predominantly up-regulates the expression of these genes, as shown by RNA sequencing (RNA-seq), messenger (mRNA) expression, and protein analyses. SALL4 expression functionally increases oxidative phosphorylation, as measured by cellular oxygen consumption rate and supported by imaging and metabolite profiling. Our work shows the ability of our endogenous-isogenic combination cell-based screening methodology to successfully identify a metabolic pathway vulnerability that is therapeutically actionable with a good therapeutic index, in SALL4-expressing cancers.

Materials and Methods

Chemical-Genetic Screening

SNU-387 empty vector–, *Tg:SALL4Ai*-, and *Tg:SALL4B*-expressing isogenic cell lines were generated by transducing wild-type SNU-387 cells with empty vector, SALL4A, or SALL4B FUW-Luc-mCh-puro lentiviral constructs.[20] Cells were plated in 50 μL of RPMI culture media in 384-well white, flat-bottom plates (Corning, Corning, NY) and incubated at 37°C in a humidified atmosphere of 5% CO_2 overnight. The numbers of cells per well were 1500 for SNU-398 and 750 for SNU-387 and SNU-387 isogenic lines. After overnight incubation, 0.5 μL of 100 μmol/L drug libraries or 10 mg/mL extract libraries were added to cells with the Bravo Automated Liquid Handling Platform (Agilent, Santa Clara, CA). Cells were then incubated for 72 hours at 37°C in a humidified atmosphere of 5% CO_2 before 10 μL of CellTiter-Glo reagent was added to the wells with the MultiFlo Microplate Dispenser (BioTek, Winooski, VT). Cells were incubated at room temperature for a minimum of 10 minutes, after which luminescence readings were recorded by an Infinite M1000 Microplate Reader (Tecan, Männedorf, Switzerland).

Hepatocellular Carcinoma Sample Collection

The collection of HCC samples for research from patients with HCC was performed under domain-specific review board protocol 2011/01580, approved by the National Healthcare Group domain-specific review board, which governs research ethics in Singapore that involves patients, staff, premises, or facilities of the National Healthcare Group and any other institutions under its oversight.

Data and Materials Availability

All sequencing data have been deposited in the National Center for Biotechnology Information Gene Expression Omnibus (GEO) databases GSE114808 and GSE112729.

Results

An Endogenous-Isogenic Chemical-Genetic Screening Platform Identifies SALL4-Selective Compounds

Our SALL4-dependent chemical-genetic screening platform consists of a pair of endogenous HCC cell lines and a

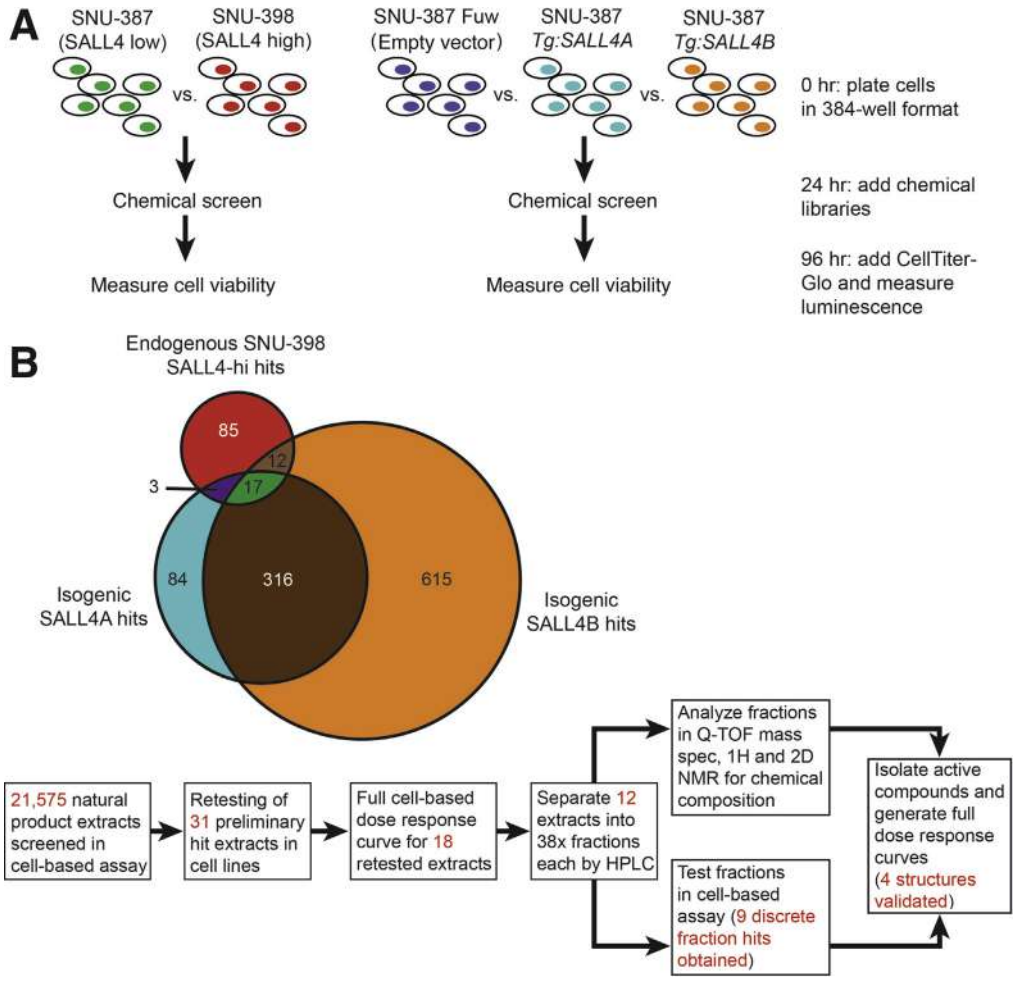

Figure 1. A chemical-genetic cell-based screening to identify compounds targeting SALL4 dependencies. (*A*) Schematic of the screening involving the use of endogenous SALL4^{lo} and SALL4^{hi} HCC lines and engineered isogenic SALL4 expressing lines. (*B*) Venn diagram illustrating the overlap of hit compounds that selectively decrease cell viability of the SALL4^{hi} lines over their respective SALL4^{lo} controls. (*C*) Workflow of natural product extract screening to identify individual compound hits from extracts containing multiple chemical entities. HPLC, high-performance liquid chromatography; hr, hour; NMR, nuclear magnetic resonance; Q-TOF, quadrupole time-of-flight.

trio of isogenic cell lines (Figure 1*A*). For the endogenous pair, SNU-398 expresses high levels of SALL4 protein, and its survival is dependent on *SALL4* expression.[14] The endogenous control SNU-387 cell line has undetectable *SALL4* RNA (Supplementary Figure 1*A*) and protein. The isogenic trio consists of lentiviral-mediated insertions into the SNU-387 SALL4 undetectable line, in which the cells are transduced with either an empty vector control or a *SALL4A*- or *SALL4B*-expressing construct (Figure 1*A*). The *SALL4*-expressing isogenic lines show SALL4 isoform-specific mRNA and protein expression (Supplementary Figure 1*B–D*) and become sensitive to *SALL4* knockdown (Supplementary Figure 1*D* and *E*). SALL4 isoform expression in these isogenic cells does not alter their growth and proliferation rates (Supplementary Figure 1*F* and *G*).

The 5 endogenous and isogenic cell lines were screened with 1597 pharmacologically active small molecules from the Selleck Anti-cancer Compound and LOPAC1280 libraries and 21,575 diverse natural product extracts of plant, fungal, and actinobacteria origin from the A*STAR Bioinformatics Institute collection.[23] Each natural product extract contains varying numbers of compounds, allowing multiplexing to achieve a screening with hundreds of thousands to millions of compounds efficiently. Cell viability was assessed after 72 hours of compound or extract incubation (Figure 1*A*). Extracts and compounds that reduced cell viability of the SALL4^{hi} cell lines (SNU-398, SNU-387 *Tg:SALL4A* and *Tg:SALL4B*) by more than 1.5-fold but had minimal effect on SALL4^{lo} (SNU-387 and SNU-387 empty vector) cell viability were identified as hits. The controls for the screening were proteasome inhibitor bortezomib, which significantly reduced cell viability of all cell lines, and the sole hit from the small-molecule library screening, PI-103, which selectively targets the SALL4^{hi} cells (Supplementary Figure 2*A*). The *Z*-factor of the screening was between 0.70 and 0.86.

We obtained thre3e categories of hits from the screening: compounds/extracts that selectively targeted endogenous SALL4^{hi} SNU-398 over SALL4^{lo} control SNU-387 (117 hits), compounds/extracts that selectively targeted *Tg:SALL4A* cells over empty vector control (420 hits), and compounds/extracts that selectively targeted *Tg:SALL4B* cells over control (960 hits) (Figure 1*B*). Each category gave at least 100 hits, but taken together, the overlapping results gave only 17 hits (1 small molecule and 16 natural product extract hits). Our combined screening methodology yields a small number of hits that conform to stringent SALL4-specificity requirements, decreasing the time and cost for further validation and workup of hits.

Because each natural product extract we screened is a mixture of compounds, we determined the specific active

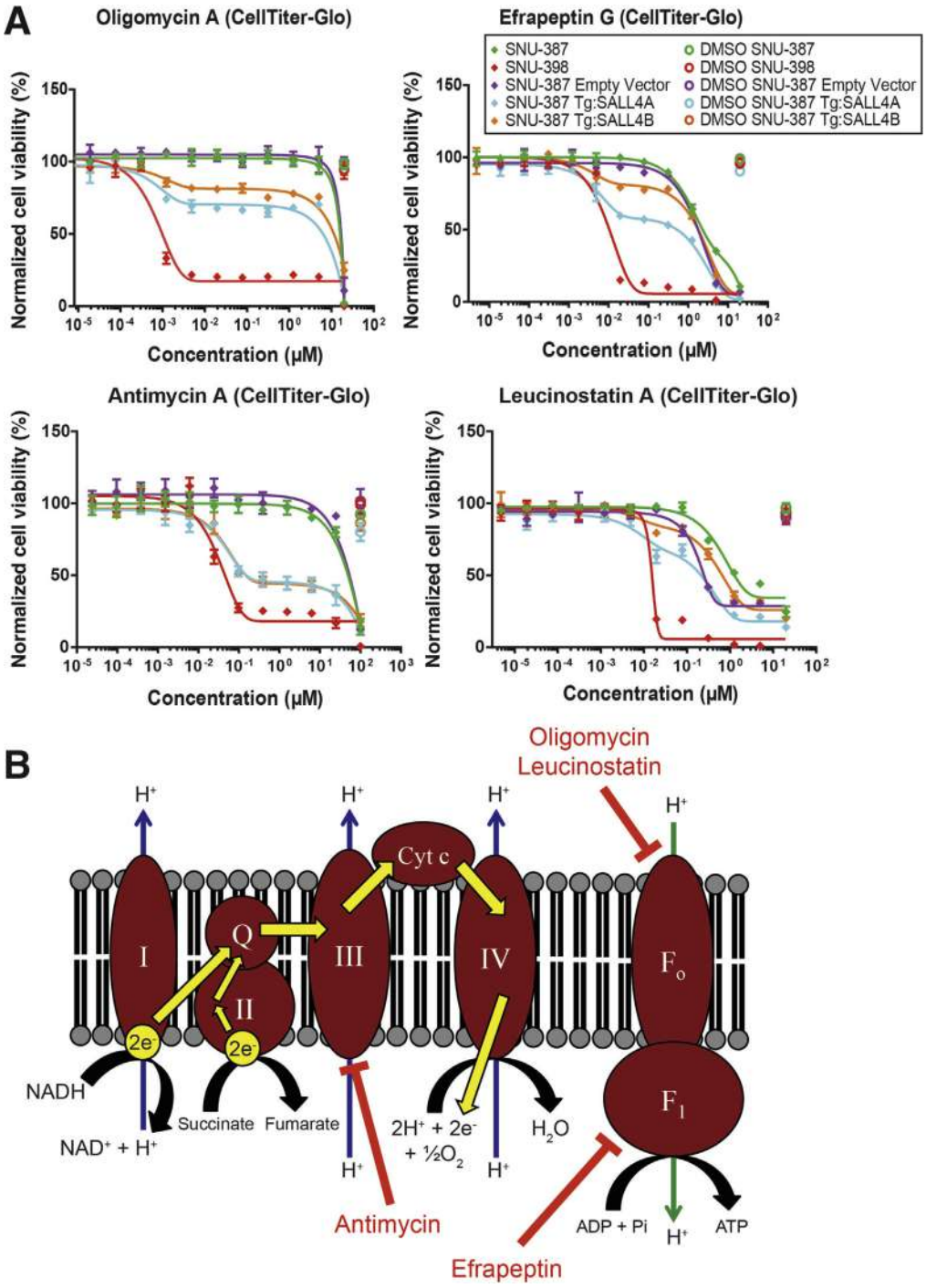

Figure 2. SALL4-dependent cells are susceptible to mitochondrial oxidative phosphorylation inhibitors. (*A*) Cell viability dose-response curves for cells treated for 96 hours with hit compounds from the natural product extract screening, oligomycin, efrapeptin, antimycin, and leucinostatin, measured with CellTiter-Glo reagent and normalized to untreated cell viability (mean of 3 replicates ± standard deviation). (*B*) Diagram indicating oxidative phosphorylation targets of validated hit compounds. M, mol/L.

components responsible for the SALL4^{hi} response. We retested 31 natural product extract hits from the Tg:SALL4A-SNU-398 overlap (3 hits), Tg:SALL4B-SNU-398 overlap (12 hits), and overlap of all 3 cell lines (16 hits) in the screening assay, and only 18 were reproducible (Figure 1*C*). These 18 hits were then validated with dose-response curves, and only 12 hits from the all-3-cell-line overlap category were validated (Figure 1*C*). No hits from the Tg:SALL4A-SNU-398 or Tg:SALL4B-SNU-398 categories passed through this validation step. Next, we fractionated the 12 validated hit extracts into 38 fractions each. Fractions were then screened to identify 9 discrete fractions that were selective for SALL4^{hi} cells, and positive fractions were subjected to quadrupole time-of-flight mass spectrometry and nuclear magnetic resonance analysis to identify active components (Figure 1*C*).

Oxidative Phosphorylation Inhibitors Target SALL4-Dependent Cell Viability

Overall, the screening identified 1 small molecule hit, PI-103, and 4 natural compound analogues, oligomycin,

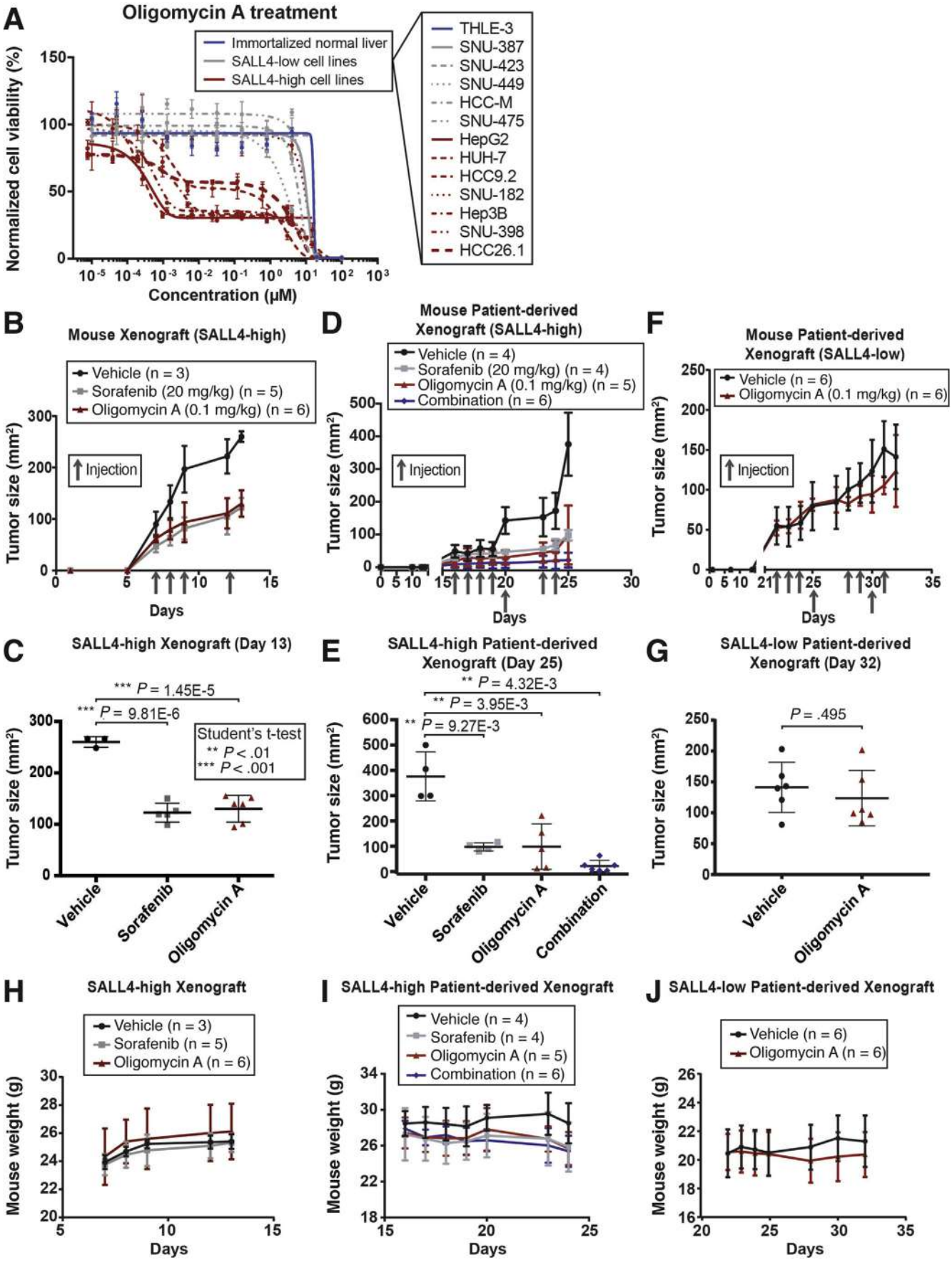
A
Oligomycin A treatment
Immortalized normal liver
SALL4-low cell lines
SALL4-high cell lines
THLE-3
SNU-387
SNU-423
SNU-449
HCC-M
SNU-475
HepG2
HUH-7
HCC9.2
SNU-182
Hep3B
SNU-398
HCC26.1
Normalized cell viability (%)
Concentration (μM)
B
Mouse Xenograft (SALL4-high)
Vehicle (n = 3)
Sorafenib (20 mg/kg) (n = 5)
Oligomycin A (0.1 mg/kg) (n = 6)
Injection
Tumor size (mm²)
Days
D
Mouse Patient-derived Xenograft (SALL4-high)
Vehicle (n = 4)
Sorafenib (20 mg/kg) (n = 4)
Oligomycin A (0.1 mg/kg) (n = 5)
Combination (n = 6)
Injection
Tumor size (mm²)
Days
F
Mouse Patient-derived Xenograft (SALL4-low)
Vehicle (n = 6)
Oligomycin A (0.1 mg/kg) (n = 6)
Injection
Tumor size (mm²)
Days
C
SALL4-high Xenograft (Day 13)
*** P = 1.45E-5
*** P = 9.81E-6
Student's t-test
** P < .01
*** P < .001
Tumor size (mm²)
Vehicle
Sorafenib
Oligomycin A
E
SALL4-high Patient-derived Xenograft (Day 25)
** P = 4.32E-3
** P = 3.95E-3
** P = 9.27E-3
Tumor size (mm²)
Vehicle
Sorafenib
Oligomycin A
Combination
G
SALL4-low Patient-derived Xenograft (Day 32)
P = .495
Tumor size (mm²)
Vehicle
Oligomycin A
H
SALL4-high Xenograft
Vehicle (n = 3)
Sorafenib (n = 5)
Oligomycin A (n = 6)
Mouse weight (g)
Days
I
SALL4-high Patient-derived Xenograft
Vehicle (n = 4)
Sorafenib (n = 4)
Oligomycin A (n = 5)
Combination (n = 6)
Mouse weight (g)
Days
J
SALL4-low Patient-derived Xenograft
Vehicle (n = 6)
Oligomycin A (n = 6)
Mouse weight (g)
Days

efrapeptin, antimycin, and leucinostatin, as being selective for SALL4^{hi} cells (Figure 2*A* and Supplementary Figure 2*A*), with a hit rate of 0.02%. Oligomycin and leucinostatin are known inhibitors of the F_0 ATP synthase subunit, efrapeptin inhibits the F_1 ATP synthase subunit, and antimycin targets cytochrome c reductase in complex III of oxidative phosphorylation[24,25] (Figure 2*B*). PI-103 has been shown to induce mitochondrial apoptosis in acute myeloid leukemia cells.[26] Because the CellTiter-Glo reagent we used for the screening quantifies ATP levels as a measure of cell viability and our hits target oxidative phosphorylation and the mitochondria, which is a major source of cellular ATP, we further validated our hits with the CyQUANT (Thermo Fisher Scientific, Waltham, MA) DNA dye as an alternative measure of cell viability. The dose response curves for the 5 hits using either CellTiter-Glo or CyQUANT were highly comparable (Supplementary Figure 2*B* and *C*). We also tested various analogues of oligomycin and efrapeptin in our cell-based assay (Supplementary Table 1*A*). The 4 natural compounds and their analogues showed potent median inhibitory concentration (IC_{50}) values in the 0.1- to 10-nmol/L range for the endogenous SALL4^{hi} SNU-398 line and partial cell viability decreases in the SALL4^{hi} isogenic lines, with selectivity ratios ranging from 200- to 20,000-fold compared with the IC_{50} values in the SALL4^{lo} control cells (Figure 1*A*, and Supplementary Figure 1*C*, and Supplementary Table 1*A*). In SALL4^{hi}cells, oligomycin A seems to induce cell death through apoptosis, as suggested by the presence of cleaved caspase-3 with oligomycin treatment in a dose response manner (Supplementary Fig 2*D*).

Oligomycin A Suppresses SALL4-Dependent Tumorigenesis

We selected oligomycin A for downstream tumor suppression and mechanistic studies because it had the most potent SALL4^{hi} cell IC_{50} of 0.5 nmol/L and the highest selectivity of 20,000-fold over the SALL4^{lo} cells. Oligomycin A is also readily available commercially. To determine if oligomycin A could selectively target other SALL4^{hi} cell lines, we performed dose response cell viability experiments on a panel of HCC cell lines. This panel includes 2 patient-derived primary cell lines, HCC9.2 and HCC26.1, from 2 Singapore patients with HCC and an immortalized normal liver cell line THLE-3 (Figure 3*A* and Supplementary Figure 3*A*). We also tested oligomycin A in a pair of non–small-cell lung cancer (NSCLC) cell lines, in which the SALL4^{hi} H661 line was previously shown to be dependent on SALL4 expression, whereas the SALL4^{lo} H1299 line was not[27] (Supplementary Figure 3*B* and *C* and Supplementary Table 1*B*). Our data suggest that oligomycin A is potent and selective against SALL4^{hi} expressing HCC and NSCLC cell lines (Figure 3*A*, Supplementary Figure 3*A*–*C*, and Supplementary Tables 1*A* and *B*).

To test the in vivo efficacy of oligomycin A in suppressing HCC tumors, we used a SALL4^{hi} mouse xenograft model of SALL4-dependent SNU-398 cells, a SALL4^{hi} patient-derived xenograft model derived from the HCC26.1 patient primary cell line expressing high levels of SALL4 (Supplementary Figure 3*A*), and a SALL4^{lo} patient-derived xenograft model of a tumor named PDX1. In the SALL4^{hi} SNU-398 cell line model, oligomycin A was able to suppress tumor size to a similar degree to the standard-of-care drug in HCC, sorafenib, but at a 200 times lower dose of 0.1 mg/kg compared with 20 mg/kg for sorafenib (Figure 3*B* and *C* and Supplementary Figure 3*D*). Similarly, oligomycin A or sorafenib treatment was able to suppress tumors in our SALL4^{hi} PDX model, with tumor suppression synergy observed with sorafenib-oligomycin combination treatment (Figure 3*D* and *E* and Supplementary Figure 3*E*). The PDX1 tumors, which showed very low SALL4 protein levels (Supplementary Figure 3*F*), did not respond to oligomycin treatment (Figure 3*F* and *G* and Supplementary Figure 3*G*). Mouse weight was not significantly affected by oligomycin treatment in all models (Figure 3*H*–*J*). We examined the known oligomycin adverse effects of muscle weakness, respiratory depression, and convulsions[28,29] in mice treated with vehicle or oligomycin over 3 weeks. To assess muscle weakness, we carried out the open field, grip strength, and rotarod tests. In the open field test, the distance traveled by the mice in 30 minutes was not significantly affected, whereas their average velocity of movement was slightly decreased with oligomycin treatment (Supplementary Figure 3*H*). In the grip strength test, the normalized full body force was not significantly affected, whereas the forepaw force was slightly decreased with oligomycin treatment (Supplementary Figure 3*I*). In the rotarod test, the latency to fall of the mice was not significantly affected by oligomycin treatment (Supplementary Figure 3*J*). We did not observe any respiratory depression or convulsions in the mice. Our data suggest that the drug was not highly toxic to the mice at this therapeutic dose.

To examine a potential correlation of oxidative phosphorylation inhibition in patients, we re-examined an HCC patient data set that we previously published for SALL4

Figure 3. Oligomycin A suppresses SALL4-dependent HCC. (*A*) Cell viability dose response curves for a panel of HCC cell lines treated with oligomycin A for 72 hours, measured with CellTiter-Glo reagent and normalized to untreated cell viability (mean of 3 replicates ± SD). (*B*) Tumor size plot of SALL4^{hi} SNU-398 mouse xenografts injected intraperitoneally with vehicle, sorafenib, or oligomycin A (mean ± SD). (*C*) Plot of tumor size at day 13 of the xenograft experiments in *B* (mean ± SD). (*D*) Tumor size plot of SALL4^{hi} PDX HCC26.1 mouse xenografts injected intraperitoneally with vehicle, sorafenib, oligomycin A, or a combination of 20 mg/kg sorafenib and 0.1 mg/kg oligomycin (mean ± SD). (*E*) Plot of tumor size at day 25 of the xenograft experiments in (*D*) (mean ± SD). (*F*) Tumor size plot of SALL4^{lo} PDX1 mouse xenografts injected intraperitoneally with vehicle or oligomycin A (mean ± SD). (*G*) Plot of tumor size at day 32 of the xenograft experiments in *F* (mean ± SD). (*H*–*J*) Mouse weight quantification plot from the respective mouse xenograft experiments in *B*–*G* (mean ± SD). M, mol/L; SD, standard deviation.

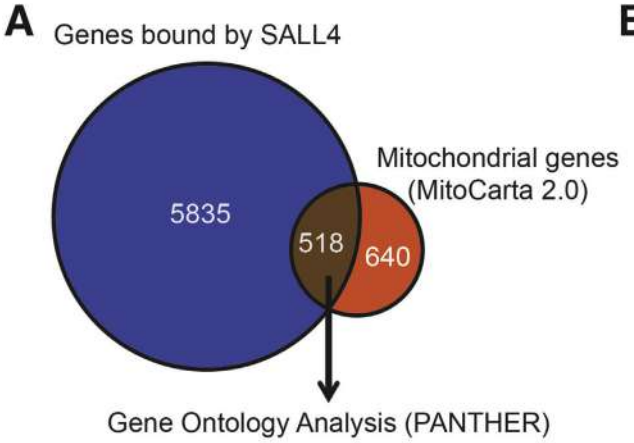

Pathway	Number of genes	Fold enrichment	*P* value	FDR
Cellular respiration	66	15.65	3.1E-51	8.0E-48
Electron transport chain	58	12.77	5.4E-41	5.6E-38
Oxidative phosphortylation	46	15.49	1.1E-35	4.5E-33

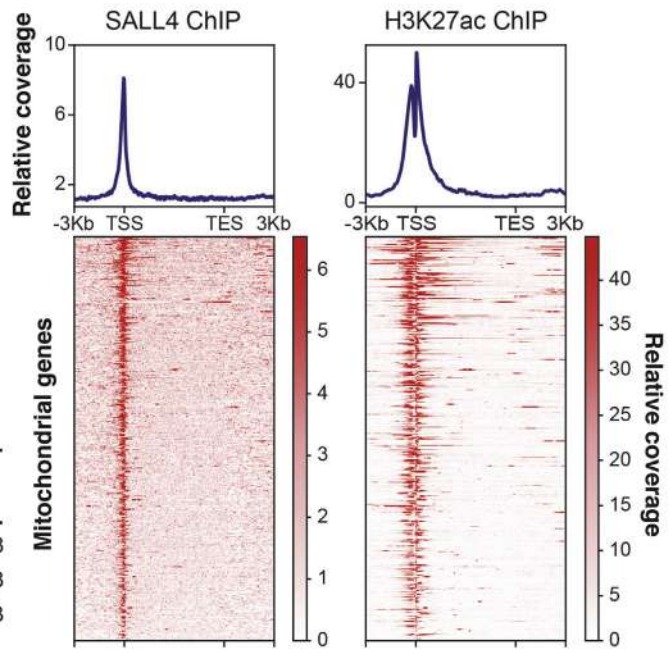

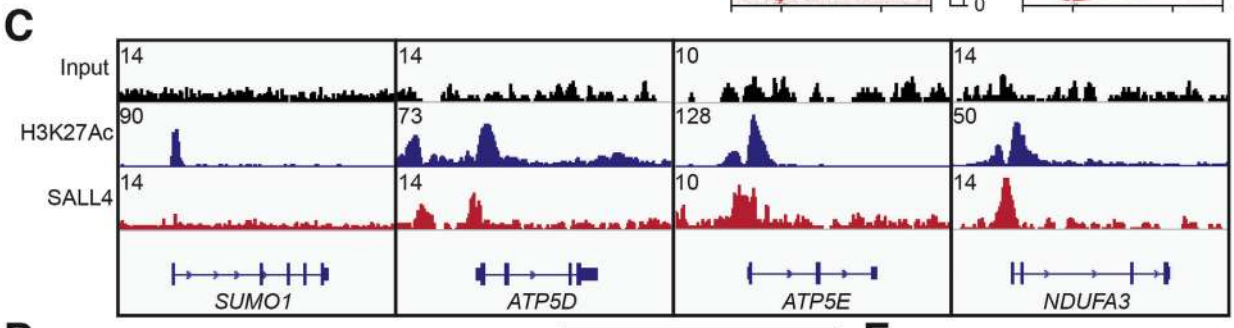

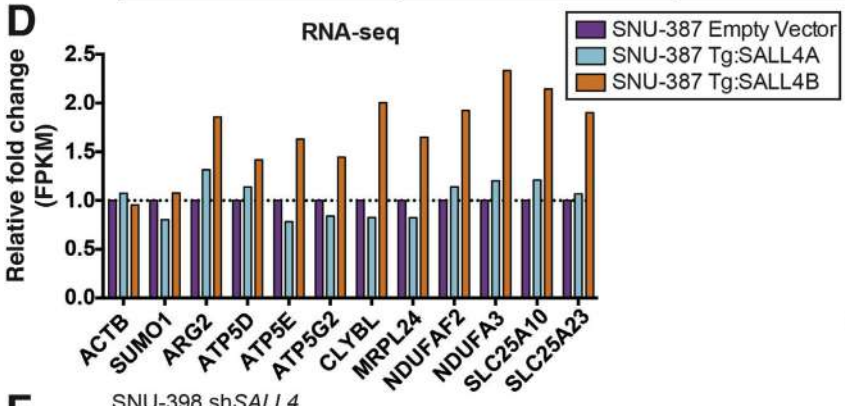

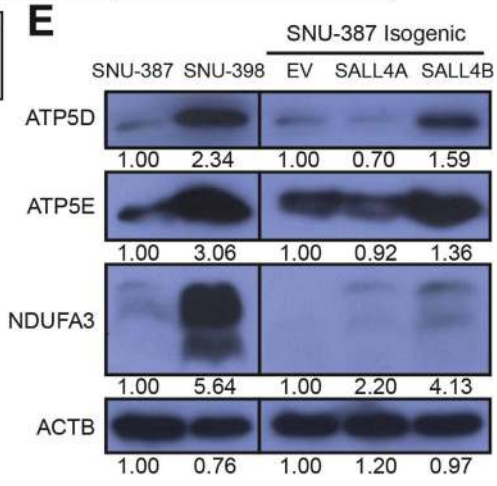

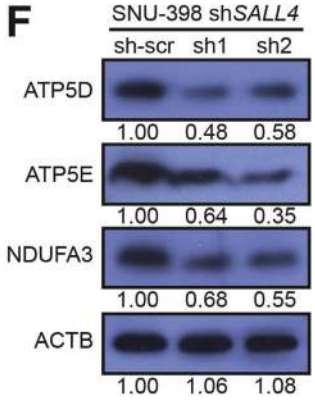

expression.[14,30] The first-line treatment for type 2 diabetes is the biguanide drug metformin, which has been shown to inhibit oxidative phosphorylation.[31,32] We previously observed that 60% of HCC patient tumors had detectable levels of SALL4, but when we stratified patients with and without diabetes, we noticed a significant difference (Supplementary Figure 3*K*). Nondiabetic patients showed the same trend of 60% SALL4 positivity as all patients combined; however, the trend was reversed in patients with diabetes, with only 40% having SALL4-positive tumors (Supplementary Figure 3*K*). Patient information on the type of diabetes and metformin use is unavailable, so more clinical work is needed to validate this correlation. We tested phenformin, an analogue of metformin with known oxidative phosphorylation inhibition activity,[32] in our SALL4 isogenic cell lines. We observed partial sensitivity to phenformin in the SALL4-expressing cells compared with the parental SALL4^{lo} line, but the effect was not as prominent as that of oligomycin A (Supplementary Figure 3*L*). The lower effectiveness of phenformin is expected because it is a less potent inhibitor of oxidative phosphorylation (IC_{50} on the order of mmol/L)[32] compared with oligomycin A (IC_{50} on the order of nmol/L).[33] Our data suggest the possibility that oxidative phosphorylation inhibition by metformin treatment in patients with diabetes suppresses SALL4-positive tumorigenesis.

Oncogenic SALL4 Binds Oxidative Phosphorylation Genes and Predominantly Up-regulates Them

Because the hits from our screening predominantly target oxidative phosphorylation, we examined our previous SALL4 and acetylated H3K27 ChIP-seq data in the SNU-398 cells.[34] We found that SALL4 binds up to 45% of mitochondrial genes, as defined by the MitoCarta 2.0 gene list, and gene ontology analysis showed that a significant number of these genes are involved in oxidative phosphorylation (Figure 4*A* and Supplementary Table 2). Gene meta-analysis of SALL4 and H3K27ac occupancy at these mitochondrial genes showed that SALL4 binds predominantly at the promoter region, between the H3K27ac double peaks[35] (Figure 4*B* and *C*).

To assess gene expression changes caused by SALL4 activity, we performed RNA-seq on the isogenic *SALL4*-expressing cells and SNU-398 SALL4^{hi} cells with *SALL4* knockdown (Supplementary Figure 4*A*). We observed that oxidative phosphorylation and other mitochondrial genes with SALL4-bound promoters show increased mRNA expression with *SALL4* expression, particularly with the *SALL4B* isoform (Figure 4*D*). In addition, *SALL4* knockdown down-regulates the expression of these genes (Supplementary Figure 4*B*). We validated the observed RNA-seq expression patterns of some of these genes by quantitative reverse-transcription polymerase chain reaction (Supplementary Figure 4*C* and *D*). Gene Set Enrichment Analysis[36] of the RNA-seq data showed significant enrichment of oxidative phosphorylation genes in the SNU-398 control compared with *SALL4* knockdown and in the SALL4B-expressing isogenic cell line compared with empty vector control (Supplementary Figure 4*E* and Supplementary Tables 3*A*–*F*). This suggests that the binding of SALL4 to oxidative phosphorylation and other mitochondrial gene promoters predominantly activates transcription of these genes. Genes that are not bound by SALL4, such as *SUMO1*, are unaffected (Figure 4*C* and *D* and Supplementary Figure 4*B*). Western blots of SALL4-bound oxidative phosphorylation genes *ATP5D*, *ATP5E*, *ATP5G2*, and *NDUFA3* and other SALL4-bound mitochondrial genes, *ARG2*, *MRPL24*, and *SLC25A23*, show similar trends in gene expression data, in which *SALL4* expression (predominantly *SALL4B*) up-regulates their protein levels, whereas *SALL4* knockdown down-regulates these levels (Figure 4*E* and *F*, Supplementary Figure 4*F* and *G*).

SALL4 Expression Functionally Increases Oxidative Phosphorylation

Because SALL4 expression in our HCC cell lines enhances oxidative phosphorylation gene mRNA and protein expression, we examined if these changes would result in functional alterations in oxidative phosphorylation. We first measured the oxygen consumption rate (OCR) of the SALL4^{hi} and SALL4^{lo} cells used in the screening, because oxidative phosphorylation requires oxygen. We observed that the OCR is significantly increased in the SNU-398 SALL4^{hi} line and by expressing either *SALL4A* or *SALL4B* in the isogenic lines (Figure 5*A*). The opposite occurs with *SALL4* knockdown in SNU-398 cells, in which OCR decreases proportionally with decreasing SALL4 protein levels, because shSALL4-2 reduces SALL4 protein level to a greater degree than shSALL4-1 (Figure 5*B* and Supplementary

Figure 4. SALL4 binds and up-regulates oxidative phosphorylation gene expression. (*A*) Venn diagram of mitochondrial genes from the MitoCarta 2.0 data set bound by SALL4 from our prior SALL4 ChIP-seq experiment performed on SNU-398 cells.[34] Selected significant pathways from Gene Ontology analysis of the SALL4-bound genes are shown. (*B*) ChIP-seq region plots of the SALL4-bound mitochondrial genes in *A*, representing the regions bound by SALL4 and marked by H3K27ac in SNU-398 cells (from analysis of prior data), −3 kb upstream of the transcription start site (TSS) and +3 kb downstream of the transcription end site (TES). (*C*) Representative ChIP-seq input, H3K27ac, and SALL4 peaks for control gene *SUMO1* and electron transport chain genes *ATP5D*, *ATP5E*, and *NDUFA3*. (*D*) RNA-seq expression level fold change for a panel of mitochondrial genes from the SALL4 bound list in *A*, in the SALL4-expressing cell lines, normalized to expression levels in the empty vector control, performed in singlet. (*E*) Western blots for SALL4-bound oxidative phosphorylation genes and ACTB loading control in the cell lines used in the screening. Bands were quantified by densitometry with SNU-387 and EV bands as references. (*F*) Western blots for the genes in *E* with *SALL4* knockdown for 72 hours in the SNU-398 cell line. Bands were quantified by densitometry with sh-scr bands as reference. EV, empty vector; FDR, false discovery rate; kb, kilo base pair; Pval, *P* value.

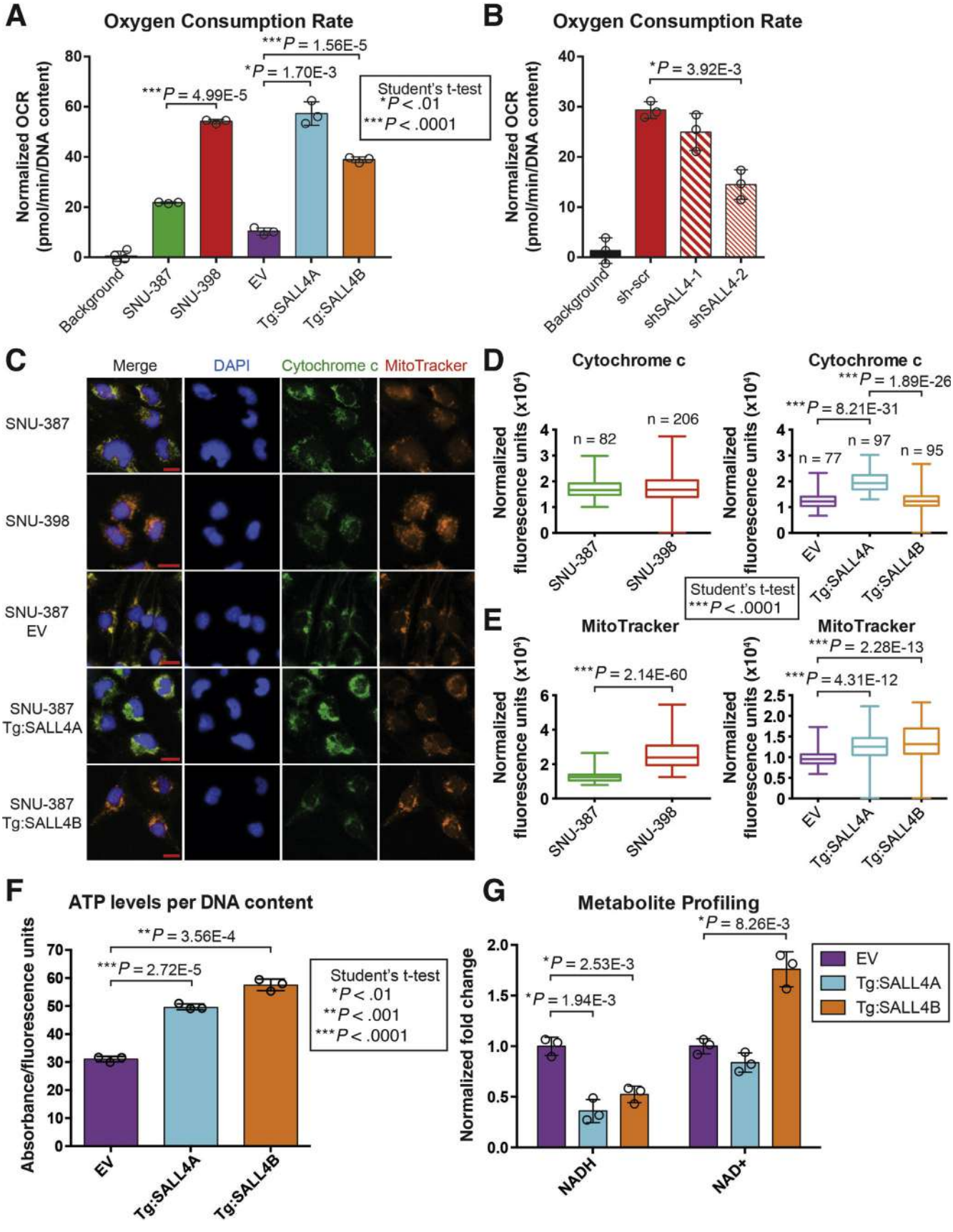
A
Oxygen Consumption Rate
Normalized OCR (pmol/min/DNA content)
***P = 1.56E-5
*P = 1.70E-3
***P = 4.99E-5
Student's t-test
*P < .01
***P < .0001
Background
SNU-387
SNU-398
EV
Tg:SALL4A
Tg:SALL4B
B
Oxygen Consumption Rate
Normalized OCR (pmol/min/DNA content)
*P = 3.92E-3
Background
sh-scr
shSALL4-1
shSALL4-2
C
Merge
DAPI
Cytochrome c
MitoTracker
SNU-387
SNU-398
SNU-387 EV
SNU-387 Tg:SALL4A
SNU-387 Tg:SALL4B
D
Cytochrome c
Normalized fluorescence units (x10⁴)
n = 82
n = 206
SNU-387
SNU-398
Cytochrome c
***P = 1.89E-26
***P = 8.21E-31
n = 77
n = 97
n = 95
EV
Tg:SALL4A
Tg:SALL4B
Student's t-test
***P < .0001
E
MitoTracker
***P = 2.14E-60
***P = 2.28E-13
***P = 4.31E-12
F
ATP levels per DNA content
Absorbance/fluorescence units
**P = 3.56E-4
***P = 2.72E-5
Student's t-test
*P < .01
**P < .001
***P < .0001
G
Metabolite Profiling
Normalized fold change
*P = 8.26E-3
*P = 2.53E-3
*P = 1.94E-3
NADH
NAD+
EV
Tg:SALL4A
Tg:SALL4B

Figure 4*G*). This suggests that *SALL4* expression increases oxidative phosphorylation-dependent OCR.

To assess mitochondrial localization and the mitochondrial membrane potential gradient generated by oxidative phosphorylation, we performed immunofluorescence imaging of the SALL4 endogenous and isogenic cell lines with oxidative phosphorylation membrane protein cytochrome c and MitoTracker (Thermo Fisher Scientific, Waltham, MA) dye, a dye that localizes to the mitochondrial membrane in a membrane potential–dependent manner (Figure 5*C*). Quantification of the fluorescence signals per cell showed that cytochrome c is significantly up-regulated in the SALL4A-expressing cells (Figure 5*D*). In addition, the MitoTracker signal is significantly increased in the SNU-398– and both *SALL4A*- and *SALL4B*-expressing cells (Figure 5*E*). These results suggest that *SALL4* expression increases oxidative phosphorylation–dependent mitochondrial membrane potential.

Because oxidative phosphorylation is functionally increased by SALL4 expression, we analyzed the levels of oxidative phosphorylation–related metabolites. We first measured ATP levels normalized to DNA content in the SALL4-expressing cells and found that ATP levels are significantly increased in both the *SALL4A*- and *SALL4B*-expressing lines (Figure 5*F*). We also performed metabolite profiling on the SALL4-expressing lines, and through Metabolite Set Enrichment Analysis,[37] we observed that electron transport chain (oxidative phosphorylation) and malate-aspartate shuttle metabolites are significantly altered in both *SALL4A* and *SALL4B* expression (Supplementary Figure 5*A* and *B*). The malate-aspartate shuttle facilitates the transfer of electrons from membrane-impermeable reduced nicotinamide adenine dinucleotide (NADH) generated during glycolysis in the cytosol to mitochondrial oxidative phosphorylation.[38] NADH levels are significantly lower in the *SALL4*-expressing lines, whereas NAD^+ levels are significantly higher, implying that there is an increased conversion of NADH into NAD^+ by oxidative phosphorylation complex I (Figure 5*G*). Malate-aspartate shuttle metabolites are also significantly increased, suggesting an increase in the transfer of electrons (NADH) generated in glycolysis to oxidative phosphorylation (Supplementary Figure 5*C*). Our metabolite profiling data imply that *SALL4* expression increases the use of oxidative phosphorylation–related metabolites to generate more ATP.

Many cancers show the Warburg effect, where glycolysis is up-regulated by the phosphoinositide 3-kinase (PI3K)/mammalian target of rapamycin (mTOR) signaling pathway.[39] Our small-molecule SALL4-selective hit from the screening, PI-103, is a pan PI3K inhibitor (Supplementary Figure 2*A*). Therefore, we examined the effects of SALL4 expression on glycolysis in our oxidative phosphorylation–dependent model. From our metabolite profiling data, glycolytic metabolites are primarily down-regulated with SALL4 expression (Supplementary Figure 5*D*). The levels of L-lactate, the end product of anaerobic respiration, were unchanged with SALL4 expression (Supplementary Figure 5*E*). Furthermore, we measured the extracellular acidification rate of the SALL4 isogenic cell lines, which measures lactate being secreted into the extracellular environment, and observed a slight decrease in the extracellular acidification rate with SALL4 expression (Supplementary Figure 5*F*). In the glycolysis stress test, we observed a marked decrease in glycolytic rate and a slight decrease in glycolytic capacity in the SALL4-expressing cells (Supplementary Figure 5*G*). To ascertain if PI3K inhibition is important for SALL4 selectivity, we tested a number of PI3K isoform-specific and mTOR inhibitors in our endogenous and isogenic cell lines. However, most of these inhibitors did not recapitulate the specificity for SALL4-expressing lines observed with PI-103 treatment (Supplementary Figure 6*A*). The SALL4-selectivity of PI-103 could be due to an off-target effect, rather than to modulation of the PI3K pathway. From these experiments, it is likely that SALL4 expression in cancer neither initiates the Warburg effect nor creates a dependency on glycolysis.

Interestingly, the top altered metabolic pathway due to SALL4 expression was the urea cycle (Supplementary Figure 5*A* and *B*). We observed significant up-regulation of urea cycle metabolites, particularly in the SALL4B-expressing cells, in our metabolite profiling data (Supplementary Figure 7*A*). When we examined our ChIP-seq data for urea cycle genes, we observed SALL4 binding only at the promoter region of *ARG2* (Supplementary Figure 7*B*). This suggests a possible coupling of oxidative phosphorylation and the urea cycle through *ARG2* regulation by SALL4. However, because SALL4 binds only 1 gene in the urea cycle, it is unlikely that the urea cycle plays a direct role in SALL4-dependent cancer.

We also examined mitochondrial DNA (mtDNA) copy number through quantitative reverse-transcription polymerase chain reaction analysis with mtDNA gene-specific primers[40] and found that the examined mtDNA regions are significantly amplified in SNU-398 $SALL4^{hi}$ cells and

Figure 5. SALL4 expression up-regulates oxidative phosphorylation. (*A*) OCR measurements of SALL4 endogenous and isogenic lines used in the screening, normalized to DNA content measured by CyQUANT reagent (mean of 3 replicates ± SD). (*B*) OCR measurements for *SALL4* knockdown in SNU-398 endogenous $SALL4^{hi}$ cells, normalized to DNA content measured by CyQUANT reagent (mean of 3 replicates ± SD). (*C*) Representative images of SALL4 endogenous and isogenic cell lines stained with 4′,6′-diamidino-2-phenylindole (DAPI) nuclear dye and MitoTracker Red mitochondrial membrane potential dye and immunostained with cytochrome c antibody. Scale bars are 20 μm in length. (*D*) Quantification of cytochrome c fluorescence signal per cell, normalized to DAPI signal (median, quartile, and range). (*E*) Quantification of MitoTracker fluorescence signal per cell, normalized to DAPI signal (median, quartile, and range). (*F*) ATP levels per DNA content for the SALL4 isogenic cell lines measured by CellTiter-Glo ATP detection reagent values normalized to CyQUANT DNA quantification reagent values (mean of 3 replicates ± SD). (*G*) NADH/NAD^+ values measured by HPLC–mass spectrometry metabolite profiling of the SALL4 isogenic cell lines (mean of 3 replicates ± SD). HPLC, high-performance liquid chromatography; SD, standard deviation.

SALL4-expressing isogenic lines (Supplementary Figure 7*C*). This suggests that SALL4 expression promotes an increase in mtDNA copy number in relation to increased oxidative phosphorylation functionality in the mitochondria. We also examined the expression of mitochondrial biogenesis regulators *PGC-1α*, *PGC-1β*, *TFAM*, *NRF1*, and *NRF2*[41–43] in our SALL4-expressing isogenic lines. Only *PGC-1α* was significantly up-regulated in the SALL4B-expressing line, and there were no appreciable alterations in *TFAM*, *NRF1*, and *NRF2* (Supplementary Figure 7*D*). *PGC-1β* expression was not detected in these lines. In our ChIP-seq data, SALL4 binding was observed only at the promoters of *NRF2* and *TFAM* (Supplementary Figure 7*E*). Our data suggests that SALL4 does not directly regulate the expression of mitochondrial biogenesis genes.

Discussion

A Combined Chemical-Genetic Screening to Discover Oncogenic Transcription Factor Vulnerabilities as Precision Medicine

Our chemical-genetic screening platform with endogenous and isogenic SALL4-expressing HCC cell lines allows for the efficient and stringent identification of a small number of hits that target both the endogenous and isogenic SALL4^{hi} lines, increasing the likelihood that these hits are specifically affecting SALL4-related biology. The endogenous pair gives biological relevance, and the isogenic trio controls for genetic background. Our combination endogenous-isogenic screening is therefore able to identify compounds that target SALL4-specific biology in a biologically relevant fashion. The 4 natural compound hits identified target different oxidative phosphorylation components, and by doing so, they potently and selectively target *SALL4*-expressing cells in both HCC and NSCLC systems. We show that ATP synthase inhibitor oligomycin A effectively targets SALL4^{hi} cells in a panel of HCC cell lines and can suppress tumors in vivo to a similar degree as the current standard-of-care drug sorafenib. Oligomycin and sorafenib also act in synergy to suppress tumorigenesis when combined. This suggests that our system can identify tool compounds that are specific to transcription factor cancer biology efficiently and effectively. Our proof-of-concept screening could have important implications for future academic studies of oncogenic transcription factor downstream pathways and potential precision medicine applications.

A Previously Unknown Metabolic Role of SALL4 in Tumorigenesis

From prior work, the widely accepted role of transcription factor SALL4 in cancer has been to modulate the expression of both procancer and anticancer genes, such as by recruiting the NuRD complex to chromatin to silence PTEN or by directly up-regulating oncogene MYC levels.

To our knowledge, our screening results and subsequent investigation into the altered processes in SALL4-dependent tumorigenesis show a previously unknown metabolic reprogramming function of SALL4. We show that SALL4 binds a significant number of oxidative phosphorylation and other mitochondrial genes at their promoters and predominantly up-regulates their mRNA expression. This gene expression up-regulation ultimately leads to increased protein levels of these genes. *SALL4* expression also leads to a functional increase in oxidative phosphorylation, with increased cellular OCR, mitochondrial membrane potential, oxidative phosphorylation–related metabolites, and mtDNA copy number. Because SALL4 expression in our isogenic cell lines does not affect cell proliferation, we believe that oxidative phosphorylation is specifically co-opted by SALL4 misexpression in cancer and not as a result of an increased proliferation rate up-regulating nonspecific housekeeping processes. Our work proposes that *SALL4* expression in cancer confers a dependency on oxidative phosphorylation through direct gene expression regulation, although the underlying preference for this metabolic reprogramming in tumorigenesis is still unclear.

We did not observe the Warburg effect, the preference for cancers to up-regulate anaerobic glycolysis for energy, in our *SALL4*-expressing cancer cell models. Recent studies have challenged the hypothesis that the Warburg effect is cancer specific, suggesting that the effect is a result of metabolic changes associated with a proliferative state rather than a unique feature of malignancy.[44] Many nonmalignant cells use the Warburg effect to proliferate. There are many advantages of non-Warburg aerobic respiration to proliferating cells, such as the supply of large quantities of anabolic precursors such as nucleotides, proteins, and lipids. Many tumor cells have been shown to use the tricarboxylic acid cycle and oxidative phosphorylation to generate ATP and balance reactive oxygen species.[45] Tumorigenesis has also been shown to be dependent on mitochondrial function. Cancer cells can use fatty acids and amino acids, rather than glucose, to supply intermediates for the trichloroacetic acid cycle and maintain mitochondrial respiration, particularly during changes in the tumor microenvironment.[30,46] This might explain why SALL4-expressing cells up-regulate oxidative phosphorylation to become tumorigenic, thereby becoming sensitive to oxidative phosphorylation inhibitors, rather than showing the Warburg effect.

Other than being a potent oncogene, SALL4 is an important developmental gene in fetal liver and in stem cells. It would be interesting to determine if oxidative phosphorylation and other metabolic processes are similarly regulated by homeostatic SALL4 expression in the developing embryo or the stem cell compartment during liver regeneration after injury. The role of SALL4 in liver regeneration is poorly understood, and future studies are needed to comprehend this role in greater detail.

SALL4 as a Potential Biomarker for Oxidative Phosphorylation Precision Medicine in Cancer

Clinical trials have been conducted to assess the effectiveness of oxidative phosphorylation inhibitors as effective cancer therapies.[47] However, the direct molecular mechanisms of oxidative phosphorylation up-regulation in cancer

are not well understood, particularly in liver cancer. This, coupled with the toxicity associated with targeting a ubiquitous cellular pathway, currently make these inhibitors less appealing as cancer drugs.

Our study shows the possibility that SALL4 can be used as a companion biomarker to select patients with cancer who may benefit from oxidative phosphorylation inhibitors in the clinic. Mechanistically, we propose a direct link between SALL4 up-regulation and an increase in oxidative phosphorylation, where SALL4 binds and transcriptionally activates oxidative phosphorylation genes during tumorigenesis. Tumors that express significant levels of SALL4 are more sensitive to oxidative phosphorylation inhibition at very low doses, as we have shown both in vitro and in vivo. A larger therapeutic window for clinical oxidative phosphorylation inhibitors is therefore possible in patients harboring SALL4-expressing tumors. Targeting SALL4-dependent cancer with oxidative phosphorylation inhibitors could lead to an effective suppression of tumorigenesis with minimal toxicity. The patient data we examined shows promise for precision medicine use of oxidative phosphorylation inhibitors in SALL4 patients, but the limitations of the annotated patient biodata, the small sample size, and the low potency of biguanides as oxidative phosphorylation inhibitors, means that more clinical studies are needed to confirm the clinical utility of our findings.

A limitation of our study is that we did not obtain SALL4A- and SALL4B-specific hits. Further studies are needed to determine the unique mechanisms by which each isoform drives cancer. A confounding issue is that SALL4A and SALL4B are coexpressed from the same gene locus as splice isoforms[15] and, from prior work, are always coexpressed in the same cell line or tumor tissue.[14,20,27] Our study shows that both SALL4 isoforms can functionally up-regulate, and thus create a dependency on, oxidative phosphorylation. Targeting this pathway shared by both isoforms with oxidative phosphorylation inhibitors is therefore a viable therapeutic option for SALL4-expressing cancers. We have observed that SALL4 is up-regulated in about 20%–30% of all solid tumors,[12,14] so the potential clinical utility of oxidative phosphorylation inhibitors with a companion SALL4 diagnostic is highly significant.

Our study shows that a SALL4 biomarker can be used in conjunction with oligomycin, a highly potent oxidative phosphorylation inhibitor that has not yet been tested extensively in clinical trials to our knowledge. The lethal dose of oligomycin that kills 33% of rats is 0.5 mg/kg (1 mg/kg for mice), whereas 100% of rats survived with 0.1 mg/kg of the drug (0.2 mg/kg for mice).[28,48] Our study dosed mice at the sublethal dose of 0.1 mg/kg oligomycin, which is 10 times less than the lethal dose that kills 335, and we observe significant and selective tumor size suppression in SALL4^{hi} tumors with low toxicity. It might be worthwhile to explore the clinical use of oligomycin in SALL4-expressing tumors.

Supplementary Material

Note: To access the supplementary material accompanying this article, visit the online version of *Gastroenterology* at www.gastrojournal.org, and at https://doi.org/10.1053/j.gastro.2019.08.022.

References

1. Patel MN, Halling-Brown MD, Tym JE, et al. Objective assessment of cancer genes for drug discovery. Nat Rev Drug Discov 2013;12:35–50.
2. Zheng W, Thorne N, McKew JC. Phenotypic screens as a renewed approach for drug discovery. Drug Discov Today 2013;18:1067–1073.
3. Wilding JL, Bodmer WF. Cancer cell lines for drug discovery and development. Cancer Res 2014;74:2377–2384.
4. Janzen WP. Screening technologies for small molecule discovery: the state of the art. Chem Biol 2014;21:1162–1170.
5. Ferlay J, Soerjomataram I, Dikshit R, et al. Cancer incidence and mortality worldwide: sources, methods and major patterns in GLOBOCAN 2012. Int J Cancer 2015;136:E359–E386.
6. Bruix J, Raoul J-L, Sherman M, et al. Efficacy and safety of sorafenib in patients with advanced hepatocellular carcinoma: subanalyses of a phase III trial. J Hepatol 2012;57:821–829.
7. Bruix J, Qin S, Merle P, et al. Regorafenib for patients with hepatocellular carcinoma who progressed on sorafenib treatment (RESORCE): a randomised, double-blind, placebo-controlled, phase 3 trial. Lancet 2017;389(10064):56–66.
8. de Celis JF, Barrio R. Regulation and function of spalt proteins during animal development. Int J Dev Biol 2009;53:1385–1398.
9. Tatetsu H, Kong NR, Chong G, et al. SALL4, the missing link between stem cells, development and cancer. Gene 2016;584:111–119.
10. **Zhang J, Tam W-L, Tong GQ**, et al. Sall4 modulates embryonic stem cell pluripotency and early embryonic development by the transcriptional regulation of *Pou5f1*. Nat Cell Biol 2006;8:1114–1123.
11. **Lim CY, Tam W-L, Zhang J**, et al. Sall4 regulates distinct transcription circuitries in different blastocyst-derived stem cell lineages. Cell Stem Cell 2008;3:543–554.
12. **Nicolè L, Sanavia T**, Veronese N, et al. Oncofetal gene SALL4 and prognosis in cancer: a systematic review with meta-analysis. Oncotarget 2017;8:22968–22979.
13. **Oikawa T, Kamiya A, Kakinuma S**, et al. Sall4 regulates cell fate decision in fetal hepatic stem/progenitor cells. Gastroenterology 2009;136:1000–1011.
14. Yong KJ, Gao C, Lim JSJ, et al. Oncofetal gene *SALL4* in aggressive hepatocellular carcinoma. N Engl J Med 2013;368:2266–2276.
15. Rao S, Zhen S, Roumiantsev S, et al. Differential roles of Sall4 isoforms in embryonic stem cell pluripotency. Mol Cell Biol 2010;30:5364–5380.
16. Kohlhase J, Chitayat D, Kotzot D, et al. *SALL4* mutations in Okihiro syndrome (Duane-radial ray syndrome), acro-

renal-ocular syndrome, and related disorders. Hum Mutat 2005;26:176–183.
17. Elling U, Klasen C, Eisenberger T, et al. Murine inner cell mass-derived lineages depend on Sall4 function. Proc Natl Acad Sci U S A 2006;103:16319–16324.
18. Yang J, Gao C, Chai L, et al. A novel SALL4/OCT4 transcriptional feedback network for pluripotency of embryonic stem cells. PLoS One 2010;5(5):e10766.
19. **Lu J, Jeong H-W**, Jeong H, et al. Stem cell factor SALL4 represses the transcriptions of PTEN and SALL1 through an epigenetic repressor complex. PLoS One 2009; 4(5):e5577.
20. Li A, Jiao Y, Yong KJ, et al. SALL4 is a new target in endometrial cancer. Oncogene 2015;34:63–72.
21. Li A, Yang Y, Gao C, et al. A SALL4/MLL/HOXA9 pathway in murine and human myeloid leukemogenesis. J Clin Invest 2013;123:4195–4207.
22. Ma Y, Cui W, Yang J, et al. *SALL4,* a novel oncogene, is constitutively expressed in human acute myeloid leukemia (AML) and induces AML in transgenic mice. Blood 2006;108:2726–2735.
23. Ng SB, Kanagasundaram Y, Fan H, et al. The 160K Natural Organism Library, a unique resource for natural products research. Nat Biotechnol 2018;36:570–573.
24. Slater EC. The mechanism of action of the respiratory inhibitor, antimycin. Biochim Biophys Acta 1973; 301:129–154.
25. Hong S, Pedersen PL. ATP synthase and the actions of inhibitors utilized to study its roles in human health, disease, and other scientific areas. Microbiol Mol Biol Rev 2008;72:590–641.
26. Park S, Chapuis N, Bardet V, et al. PI-103, a dual inhibitor of Class IA phosphatidylinositide 3-kinase and mTOR, has antileukemic activity in AML. Leukemia 2008; 22:1698–1706.
27. **Yong KJ, Li A, Ou W-B**, et al. Targeting SALL4 by entinostat in lung cancer. Oncotarget 2016;7:75425–75440.
28. Kramar R, Hohenegger M, Srour AN, et al. Oligomycin toxicity in intact rats. Agents Actions 1984;15:660–663.
29. Smith RM, Peterson WH, McCoy E. Oligomycin, a new antifungal antibiotic. Antibiot Chemother 1954;4:962–970.
30. Lu G-D, Ang YH, Zhou J, et al. CCAAT/enhancer binding protein α predicts poorer prognosis and prevents energy starvation–induced cell death in hepatocellular carcinoma. Hepatology 2015;61:965–978.
31. Holman R. Metformin as first choice in oral diabetes treatment: the UKPDS experience. Journ Annu Diabetol Hotel Dieu 2007;2007:13–20.
32. Bridges HR, Jones AJY, Pollak MN, et al. Effects of metformin and other biguanides on oxidative phosphorylation in mitochondria. Biochem J 2014;462:475–487.
33. Fang M, Qu Y, Gao B, et al. Oligomycin, a complex V inhibitor, decreases left ventricular contractility in isolated rabbit heart. FASEB J 2011;25:lb362.
34. **Liu BH, Jobichen C**, Chia CSB, et al. Targeting cancer addiction for SALL4 by shifting its transcriptome with a pharmacologic peptide. Proc Natl Acad Sci U S A 2018; 115:E7119–E7128.
35. **Wang Z, Zang C, Rosenfeld JA**, et al. Combinatorial patterns of histone acetylations and methylations in the human genome. Nat Genet 2008;40:897–903.
36. **Subramanian A, Tamayo P**, Mootha VK, et al. Gene set enrichment analysis: a knowledge-based approach for interpreting genome-wide expression profiles. Proc Natl Acad Sci U S A 2005;102:15545–15550.
37. Xia J, Wishart DS. MSEA: a web-based tool to identify biologically meaningful patterns in quantitative metabolomic data. Nucleic Acids Res 2010;38(Web server issue):W71–W77.
38. Lu M, Zhou L, Stanley WC, et al. Role of the malate-aspartate shuttle on the metabolic response to myocardial ischemia. J Theor Biol 2008;254:466–475.
39. Courtnay R, Ngo DC, Malik N, et al. Cancer metabolism and the Warburg effect: the role of HIF-1 and PI3K. Mol Biol Rep 2015;42:841–851.
40. Phillips NR, Sprouse ML, Roby RK. Simultaneous quantification of mitochondrial DNA copy number and deletion ratio: a multiplex real-time PCR assay. Sci Rep 2014;4:3887.
41. Mendham AE, Duffield R, Coutts AJ, et al. Similar mitochondrial signaling responses to a single bout of continuous or small-sided-games-based exercise in sedentary men. J Appl Physiol 2016;121:1326–1334.
42. Eisele PS, Salatino S, Sobek J, et al. The peroxisome proliferator-activated receptor γ coactivator $1\alpha/\beta$ (PGC-1) coactivators repress the transcriptional activity of NF-κB in skeletal muscle cells. J Biol Chem 2013; 288:2246–2260.
43. LeBleu VS, O'Connell JT, Gonzalez Herrera KN, et al. PGC-1α mediates mitochondrial biogenesis and oxidative phosphorylation in cancer cells to promote metastasis. Nat Cell Biol 2014;16:992–1003.
44. Vander Heiden MG, DeBerardinis RJ. Understanding the intersections between metabolism and cancer biology. Cell 2017;168:657–669.
45. DeBerardinis RJ, Chandel NS. Fundamentals of cancer metabolism. Sci Adv 2016;2(5):e1600200.
46. Palm W, Thompson CB. Nutrient acquisition strategies of mammalian cells. Nature 2017;546(7657):234–242.
47. Ashton TM, McKenna WG, Kunz-Schughart LA, et al. Oxidative phosphorylation as an emerging target in cancer therapy. Clin Cancer Res 2018;24:2482–2490.
48. Freireich EJ, Gehan EA, Rall DP, et al. Quantitative comparison of toxicity of anticancer agents in mouse, rat, hamster, dog, monkey, and man. Cancer Chemother Rep 1966;50:219–244.

Author names in bold designate shared co-first authorship.

Received January 3, 2019. Accepted August 9, 2019.

Reprint requests
Address requests for reprints to: Daniel G. Tenen, MD, Cancer Science Institute of Singapore, 14 Medical Drive MD6 #12-01, Centre for Translational Medicine, Singapore 117599. e-mail: daniel.tenen@nus.edu.sg; fax: +65-68739664.

Acknowledgments
We thank Min Yuan for her assistance with the metabolite profiling experiments.
Author contributions: Justin L. Tan conceptualized the project and wrote the manuscript. Justin L. Tan, Feng Li, and Joanna Z. Yeo participated in data

curation, methodology, and investigation. Yoganathan Klanagasundara and Siew Bee Ng participated in investigation and provided resources. Justin L. Tan, Daniel G. Tenen, Wai Leong Tam, and Li Chai provided supervision and resources. All other authors participated in data curation and investigation.

Conflicts of interest
These authors disclose the following: Justin L. Tan, Yoganathan Kanagasundaram, Siew Bee Ng, Wai Leong Tam, Li Chai, and Daniel G. Tenen are co-inventors on a patent application filed by A*STAR A*ccelerate, the National University of Singapore, and Brigham & Women's Hospital relating to work in this manuscript. The remaining authors disclose no conflicts.

Funding
This work was supported by the Genome Institute of Singapore Innovation Fellow Award (Justin L. Tan); A*STAR A*ccelerate Gap Funding ETPL/18-GAP018-R20H (Justin L. Tan); Singapore Ministry of Health's National Medical Research Council (Singapore Translational Research [STaR] Investigator Award, Daniel G. Tenen; NMRC/OFIRG/0064/2017, Wai Leong Tam; LCG17MAY004, Wai Leong Tam; and NMRC/TCR/015-NCC/2016, Wai Leong Tam); National Research Foundation Singapore (NRF-NRFF2015-04 grant, Wai Leong Tam) and the Singapore Ministry of Education under its Research Centres of Excellence initiative; Singapore Ministry of Education Academic Research Fund Tier 3, grant number MOE2014-T3-1-006 (Daniel G. Tenen); National Institutes of Health/National Cancer Institute grant R35CA197697 (Daniel G. Tenen); National Institutes of Health/National Heart, Lung, and Blood Institute grant P01HL095489 (Li Chai); Leukemia & Lymphoma Society (LLS) grant P-TRP-5854-15 (Li Chai). This work was supported in part by the Japan Society for the Promotion of Science (JSPS) Grant-in-Aid for Scientific Research (KAKENHI) (grant numbers: JP17H05623, JP17K19603, JP18H05102, JP19H01177, and JP19H05267) (Alicia G. Stein).

Supplementary Materials and Methods

Antibodies

Western blot antibodies are ACTB from Cell Signaling Technology (4970S; Danvers, MA), ARG2 from Abcam (ab137069; Cambridge, UK), ATP5D from Abcam (ab97491), ATP5E from Santa Cruz Biotechnology (sc-393695; Dallas, TX), ATP5G2 from Abcam (ab80325), CASP3 from Cell Signaling Technology (9662), cleaved CASP3 from Cell Signaling Technology (9661S), MRPL24 from Santa Cruz Biotechnology (sc-393858), NDUFA3 from Abcam (ab68089), SALL4 from Santa Cruz Biotechnology (sc-101147), and SLC25A23 from Santa Cruz Biotechnology (sc-377109). The SALL4 antibody used for immunohistochemistry is from Santa Cruz Biotechnology (sc-101147). The antibody used for immunofluorescence is Cytochrome c from BD Biosciences (556432; Franklin Lakes, NJ).

Cell Culture

Human hepatocellular carcinoma cell lines SNU-387, SNU-398, SNU-182, SNU-423, SNU-475, SNU-449, and HCC-M, and non–small-cell lung cancer cell lines H1299 and H661 (ATCC, Manassas, VA) were grown on standard tissue culture plates in filter sterilized RPMI (Gibco, Waltham, MA) with 10% heat-inactivated fetal bovine serum (HyClone GE Healthcare, Chicago, IL), 2 mmol/L L-glutamine (Gibco), and 1% penicillin-streptomycin (Gibco). Human hepatocellular carcinoma cell lines HepG2, Hep3B, and Huh-7 (ATCC) were grown on standard tissue culture plates in filter sterilized in Dulbecco's modified Eagle medium (DMEM) (Gibco) with 10% heat-inactivated fetal bovine serum (HyClone), 2 mmol/L L-glutamine (Gibco), and 1% penicillin-streptomycin (Gibco). Human immortalized liver cell line THLE-3 was grown on standard tissue culture plates in filtered Bronchial Epithelial Cell Growth Medium with additives (Lonza, Basel, Switzerland), 10% heat-inactivated fetal bovine serum (HyClone), and 1% penicillin-streptomycin (Gibco). Cells were incubated at 37°C in a humidified atmosphere of 5% CO_2. Primary HCC cell lines HCC9.2 and HCC26.1 were cultured in a medium containing Advanced F12/DMEM reduced serum medium (1:1) (Gibco, 12643), 10 mmol/L HEPES (Gibco), 100 U/mL penicillin-streptomycin (Gibco), 2 mmol/L L-glutamine (Gibco), 1% N2 (Gibco), 2% B27 (Gibco), 50 ng/mL, epidermal growth factor (Millipore, Billerica, MA), 250 ng/mL R-Spondin1 (R&D Systems, Minneapolis, MN), and 2 μmol/L SB431542 (Tocris). The cells were cultured on standard tissue culture dish coated with 3% Matrigel (Corning, Corning, NY). Cells were incubated at 37°C in a humidified atmosphere of 5% CO_2.

Natural Product Extract Dereplication

Active extracts were subjected to a dereplication procedure as described in the literature.[1] Active fractions were analyzed by accurate mass spectrometry (MS) and tandem MS (MS/MS), and data were matched against accurate mass of natural product compounds and A*STAR containing accurate mass and MS/MS mass spectra records of compounds that have been analyzed under the same conditions. Oligomycin, 21-hydroxy oligomycin A, leucinostatin A, and antimycin A were dereplicated by this method.[1]

Fungi Strain F36017 Fermentation (Efrapeptin Producing)

F36017 *Tolypocladium niveum* is a soil fungus isolated from the United Kingdom. A 7-day-old culture of F36017 grown on malt extract agar (Oxoid, Cheshire, UK) was used to prepare 5 flasks of seed cultures, comprising of 50 mL of seed medium (yeast extract 4 g/L [Becton Dickinson, Franklin Lakes, NJ], malt extract 10 g/L [Sigma-Aldrich, St Louis, MO], glucose 4 g/L [1st Base, Singapore]; pH 5.5) placed in 250-mL Erlenmeyer flasks. These seed cultures were allowed to grow for 5 days at 24°C with shaking at 200 revolutions/minute (rpm). At the end of the incubation period, the 5 flasks of seed cultures were combined and homogenized using a rotor stator homogenizer (Omni, Kennesaw, GA). Then, 5 mL of the homogenized seed culture was used to inoculate each of the 40 flasks containing 6 g of vermiculite and 50 mL of fermentation medium (maltose 30 g/L [Sigma], glucose 10 g/L [1st Base], yeast extract 0.8 g/L [Becton Dickinson], peptone 2 g/L [Oxoid], potassium phosphate monobasic 0.5 g/L [Sigma-Aldrich], magnesium sulfate heptahydrate 0.5 g/L [Merck, Kenilworth, NJ], ferric chloride 10 mg/L [Sigma-Aldrich], zinc sulfate 2 mg/L [Merck], calcium chloride 55 mg/L [Sigma-Aldrich]; pH 6.0]. Static fermentation was carried out for 14 days at 24°C. At the end of the incubation period, the cultures from all 40 flasks were harvested and freeze dried. The dried vermiculite cakes in each flask were scrambled lightly before extracting overnight 2 times with 100 mL methanol per flask. The insoluble materials from each extraction were removed by passing the mixtures through cellulose filter paper (Whatman grade 4, GE Healthcare, Chicago, IL), and the filtrates were dried by rotary evaporation.

Efrapeptin Isolation

The culture broths (40 × 50 mL, total 2 L) of *Tolypocladium niveum* (F36017) were combined and freeze-dried and partitioned with DCM:MeOH:H_2O in a ratio of 1:1:1. The organic layer was then evaporated to dryness by using rotary evaporation. The dried dichloromethane crude extract (0.7 g) was redissolved in methanol and separated by C18 reversed-phase preparative HPLC (solvent A: H_2O plus 0.1% HCOOH; solvent B: ACN + 0.1% HCOOH; flow rate: 30 mL/minutes; gradient conditions: 70:30 isocratic for 3 minutes; 30%–40% of solvent B over 12 minutes, 30%–65% of solvent B over 60 minutes, followed by 65%–100% of solvent B over 15 minutes, and finally isocratic at 100% of solvent B for 20 minutes) to give 0.6 mg of efrapeptin D (1: room temperature, 18.5 minutes), 1.0 mg of efrapeptin Eα (2: room temperature, 20 minutes), 0.5 mg of efrapeptin G (3: room temperature, 25 minutes), and 1.0 mg of efrapeptin H (4: room temperature, 27 minutes). Efrapeptins were elucidated by comparison of accurate mass and ^{1}H nuclear magnetic resonance data to those of efrapeptins published with activity against bacteria and tumor cells.[2]

Drug Treatment

Drugs used in the study were PI-103 (Selleckchem, Houston, TX); oligomycin A (Selleckchem; LKT Labs, St Paul MN); 21-hydroxy oligomycin A (Enzo Life Sciences, Farmingdale, NY); oligomycin A, B, and C mix (Enzo Life Sciences); sorafenib tosylate (Selleckchem); bortezomib (Selleckchem); antimycin A (Sigma-Aldrich); cyclosporine A (LC Laboratories, Woburn, MA), leucinostatin A (Bioinformatics Institute NPL collection; Singapore, Natural Product Library); phenformin (Sigma-Aldrich); alpelisib (Selleckchem); SB2343 (Selleckchem); idelalisib (Selleckchem); SB2602 (MedKoo Biosciences, Morrisville, NC), CUDC-907 (Selleckchem), and TGX-221 (Selleckchem).

MTT Cell Viability Assay

The 3-(4,5-dimethylthiazol-2-yl)-2,5-diphenyltetrazolium bromide (MTT) assay was used to examine the effect of SALL4 knockdown on isogenic SNU387 cell viability. Three days after viral infection, 3000 SNU-387 cells in a volume of 200 μL were plated into 96-well plates in triplicate and incubated for the indicated time points. On the day of analysis, 20 μL of MTT solution (5 mg/mL, Sigma-Aldrich) was added, after which the plates were incubated for 2 hours at 37°C. After removal of the medium, the purple formazan crystals formed were dissolved in 100 μL dimethyl sulfoxide (DMSO) with a 100minute incubation at 37°C. The optical density of dissolved purple crystal was measured by the Safire 2 plate reader (Tecan) at a wavelength of 570 nm.

CyQUANT Cell Viability Measurements

DNA content of plated cells was measured by application of the CyQUANT Direct Cell Proliferation Kit (Thermo Fisher Scientific) that contains a cell-permeable fluorescent DNA binding dye. Cells were plated in either 96- or 384-well black, clear-bottom tissue culture plates (Greiner, Kremsmünster, Austria) and allowed to reach the appropriate confluency before the addition of the appropriate amount of CyQUANT reagent, as detailed in the manufacturer's protocol. Cells were incubated for at least 1 hour at 37°C in a humidified atmosphere of 5% CO_2, after which fluorescence readings were measured by an Infinite M1000 Microplate Reader (Tecan) within a wavelength range of 480–535 nm.

Cell Counting Kit-8 Cell Viability Measurements

Cells were cultured overnight in 96-well plates with 50 μL RPMI 1640 medium (10% fetal bovine serum) with 1250 cells per well for SNU-387 empty vector and SNU-387 parental cells and 750 cells per well for SNU387 TgSALL4A and B cells. Cells were grown overnight before drug treatment. Phenformin, at varying concentrations, was dissolved in culture media. Next, 50 μL of the solution was added to each well. After a 96-hour incubation, 10 μL of Cell Counting Kit-8 reagent (Dojindo, Rockville, MD) was added to each well. After a 4-hour incubation, optical density values were determined at a wavelength of 450 nm on a SpectraMax M3 Microplate Reader (Molecular Devices, Sunnyvale, CA).

EdU Cell Proliferation Assay

The Click-iT Plus EdU Alexa Fluor 488 Flow Cytometry Assay (Thermo Fisher Scientific) to assess cell proliferation was carried out following the manufacturer's protocol. SNU-387 isogenic lines were seeded in a 6-well plate overnight, after which the cells were incubated with 10 μmol/L Click-iT EdU for 3 hours. The cells were harvested and washed with 1% bovine serum albumin (BSA) in phosphate-buffered saline (PBS) and incubated with Click-iT fixative for 15 minutes. After fixation, the cells were washed with 1% BSA in PBS and permeabilized in Click-iT saponin-based permeabilization and wash reagent. The Click-iT reaction was then performed by incubating the cells with the Click-iT reaction cocktail for 30 minutes to label the EdU-incorporated cells with Alexa Fluor 488 dye. A standard flow cytometry method was used for determining the percentage of S-phase cells in the population by using the BD LSR II Cell Analyzer (BD Biosciences).

Cell Counts

SNU-387 isogenic cell lines growing at exponential phase were seeded in 6-well plates at a density of 1.5×10^5 cells/well. Every 3–4 days, the cells were trypsinized, after which cell numbers were counted to record the growth of the cells. Then, the cells were plated at equal cell numbers in new plates with fresh medium. Total cell number is presented as viable cells per well after split adjustment.

SALL4 Knockdown by Lentiviral Transduction

The published lenti short hairpin (sh) RNA vector pLL3.7 for scrambled (sh-scr), shSALL4-1, and shSALL4-2[3] were transfected into 293FT cells, along with packaging plasmid (psPAX2) and envelope plasmid (pMD2.G) by using jetPRIME DNA transfection reagent (Polyplus Transfection, Illkirch, France) according to the manufacturer's protocol for viral packaging. Viral supernatants were collected twice at 48 and 72 hours after transfection and filtered through 0.45-μm sterile filters. Virus stocks were concentrated by ultracentrifuge at 21,000g for 2 hours at 4°C. Viral transduction were carried out using spinoculation. Briefly, fresh medium containing lentivirus and 5 μg/mL Polybrene Infection/Transfection Reagent (Sigma-Aldrich, St Louis, Mo) were added to plated cells. The plates was then centrifuged at 800g at 37 °C for 1 hour and incubated at 37°C in a humidified atmosphere of 5% CO_2.

Scrambled: GGGTACGGTCAGGCAGCTTCTTTCAAGA GAAGAAGCTGCCTGACCGTACCCTTTTTTC

shSALL4-1: GGCCTTGAAACAAGCCAAGCTATTCAAGAGA-TAGCTTGGCTTGTTTCAAGGCCTTT TTC

shSALL4-2: TGCTATTTAGCCAAAGGCAAATTCAA GAGATTTGCCTTTGGCTAAATAGCTTTTTTC

Immunohistochemistry

Immunohistochemistry was performed using Santa Cruz SALL4 antibody (sc-101147). Slides were first

deparaffinized with xylene, 100% ethanol, 95% ethanol, 70% ethanol, and distilled water, respectively. After deparaffinization, slides were blocked for 30 minutes in blocking buffer (65 mL 100% methanol, 3.5 mL 30% hydrogen peroxide, 31.5 mL water) to block endogenous peroxidase. Subsequently, antigen retrieval was conducted in 1× pH 6 citrate buffer (Sigma-Aldrich) and boiled for 30 minutes. Slides were washed 3 times with distilled water and blocked in normal blocking serum provided by Vectastain ABC kit (Vector Laboratories Inc, Burlingame, CA) for 1 hour at room temperature. Next, slides were incubated in SALL4 primary antibody diluted 1:400 in blocking serum for 1 hour at room temperature. Before staining with secondary antibody, slides were washed 3 times in PBS with 0.1% triton-X. After staining with secondary antibody, slides were incubated in ABC reagent (from the Vectastain ABC kit) in a humidified chamber for 1 hour at room temperature after 3-times wash in PBS. Washing was carried out in PBS 3 times before detection was done with a DAB kit (Vector Laboratories, Burlingame, CA), and slides were incubated in the dark at room temperature for 5 minutes. Finally, counterstaining was performed in hematoxylin for 15 minutes and dehydration in 70% ethanol, 95% ethanol, 100% ethanol, and xylene, respectively.

Mouse Xenograft

Animals were maintained and studies were carried out according to the Institutional Animal Care and Use Committee protocols. For the SALL4^{hi} models, the SNU-398 cell line and HCC26.1 patient primary cells were cultured as detailed in the "Cell Culture" section of the Supplementary Methods. *NOD.Cg-Prkdc^{scid} Il2rg^{tm1wjl} SzJ* (NSG) mice, both male and female, were anesthetized using 2.5% isofluorane (Sigma-Aldrich), and 1,000,000 cells in 200 μL of RPMI/Primary HCC cell media + Matrigel (1:1 ratio) were injected subcutaneously per mouse flank. For the SALL4^{lo} model, the PDX1 tumor was digested with collagenase and dispase and passed through a 70 μm cell strainer (Corning, Corning, NY) to obtain a single-cell suspension in supplemented DMEM/F12 media. The suspension was treated with red blood cell lysis buffer and DNase (New England Biolabs, Ipswich, MA). After washing the cells with PBS, the suspension was mixed with an equal volume of Matrigel and injected subcutaneously in the flank of 7 female NSG mice for initial tumor propagation. The 7 PDX1 tumors were harvested after 4 weeks and processed for injection as described previously. Viable cells were counted and mixed with Matrigel to obtain a 2,500,000-cells/mL single-cell suspension, and 500,000 PDX1 cells were injected subcutaneously into the left flank of each of 12 NSG mice. Isoflurane was used to anesthetize mice during injections. Drug treatment was carried out when tumors were visible. Drugs were dissolved in vehicle, 5% DMSO (Sigma-Aldrich) and 95% corn oil (Sigma-Aldrich) and injected intraperitoneally at a dose of 20 mg/kg for sorafenib and 0.1 mg/kg for oligomycin A, with the same doses used in the combination treatment, once daily on weekdays, with no injections on weekends. Mouse weight and tumor size were recorded before each injection. Once tumors reached >1.5 cm in diameter, mice were killed, and tumors were snap frozen in liquid nitrogen.

Mouse Toxicity Testing

Female NSG mice were injected with vehicle or 0.1 mg/kg of oligomycin A 3 times a week every Monday, Wednesday, and Friday for 3 weeks, then subjected to the following assays.

Open Field Test (Locomotor Testing). Mice were transported to the procedure room at least 2 hours before experiments to allow for habituation to the novel room. Locomotor activity recordings were carried out using a square open field (40 × 40 cm) in a acrylic cage, equipped with 2 rows of photocells sensitive to infrared light. The testing apparatus was enclosed in a ventilated, quiet procedure room. Measurements were performed under low levels of light to minimize stress levels of the mice and allow for normal exploratory behavior. The mice were introduced into the locomotor cage and allowed to explore freely for 30 minutes. Locomotor activity data were collected automatically. The exploratory behaviors were also captured through video recordings. The total distance traveled over 30 minutes and the average velocity, from 6 independent measurements, were measured for each mouse.

Grip Strength Tests. These tests were performed using a grip strength meter. The forelimb and full body grips of each mouse were measured in 3 successive trials and recorded. Hindlimb measures were calculated by using the difference between the grams-force recorded for the full body and the forelimb. The results of the 3 tests were averaged for each mouse.

Rotarod Test. Mice were placed on the rotor-rod apparatus that linearly accelerated from 4 to 40 rpm at a rate of 0.1 rpm/s. Mice were tested in 4 trials, with a 15-minute rest period between tests. The latency to fall and distance traveled by each mouse were recorded.

Home Cage Recording. Each mouse was monitored in its home cage for 24 hours through video recording to capture any instances of abnormal neurologic events such as seizures.

Chromatin Immunoprecipitation Sequencing Analysis

ChIP-seq data were downloaded from the National Center for Biotechnology Information GEO with accession number GSE112729.[4] Reads were mapped by bowtie2 against human reference genome GRCh38. Polymerase chain reaction (PCR) duplicates were removed in the paired-end alignments by samtools rmdup.[5] Peak calling was performed by macs2 with default options. Annotation of the peaks was done by annotatePeaks.pl in Homer software packages.[6] Alignment files in BAM format were converted to signals by using bedtools,[7] and the average coverage of each ChIP-seq experiment was adjusted to 1. bedGraphToBigWig was used to convert the result into BigWig format files. Heatmaps were generated by Deeptools2 along regions on mitochondria genes.[8] Regions were sorted according to the strength of SALL4 signals.

RNA Sequencing

SALL4-targeting shRNA was transduced into the SNU-398 HCC cell line as previously described.[3] Three days after transduction, the cytoplasm of the cells was removed by Dounce homogenizer, and nuclear RNA was extracted by using the RNeasy Mini Kit (Qiagen, Hilden, Germany). For SNU-387 SALL4A and SALL4B-expressing isogenic cell lines, SNU-387 HCC cells were transduced with SALL4A or SALL4B FUW-Luc-mCh-puro lentiviral constructs.[9] Puromycin was used to select for stable SALL4A- or SALL4B-expressing cells. More than 2 weeks after selection, RNA was harvested from these isogenic cells using an RNeasy Mini Kit (Qiagen). The quality of the harvested total RNA was analyzed on Bioanalyzer (Agilent, Santa Clara, CA) before generation of the sequencing libraries, an RNA integrity number of >9 from all samples was observed. Complementary DNA (cDNA) library construction was then performed by using the stranded ScriptSeq Complete Gold kit (human/mouse/rat) (Epicenter; now available through Illumina, San Diego, CA). Ribosomal RNA depletion was included in the library construction steps. Paired-end 76-base-pair sequencing was done with the Illumina HiSeq 2000 sequencer. The paired-end RNA-seq reads were mapped by TopHat2 pipeline against human reference genome GRCh38 with gene annotation GENCODE 24.[10] PCR duplicates were removed in the paired-end alignments by samtools rmdup.[5] Alignments with mapping quality of <20 were also removed. Based on the reads mapped in the transcriptome, gene expression levels in FPKM were determined by cuffdiff in the Cufflinks package.[11] Gene Set Enrichment Analysis (GSEA) was performed by following the manual of the GSEA software.[12] Sequencing data have been deposited in the National Center for Biotechnology Information GEO database with accession number GSE114808.

Immunofluorescence Assay and Image Analysis

Cells were plated in 96-well black, clear-bottom plates overnight at 50%–80% confluency. The following day, MitoTracker Red CMXRos (300 nmol/L, Thermo Fisher Scientific) was added into live cells for 30 minutes at 37°C. Cells were then washed 3 times for 5 minutes in PBS and fixed in 4% PFA for 15 minutes at room temperature. After 3 washes of PBS, cells were incubated in blocking buffer (5% horse serum, 1% BSA, 0.2% Triton-X in PBS) for 1 hour at room temperature. Cytochrome-c antibody (BD Pharmigen, Franklin Lakes, NJ; clone 6H2.B4) was added at 1:1000 dilution in blocking buffer and incubated overnight at 4°C. The next day, cells were washed 3 times for 5 minutes in PBS and incubated with Alexa Fluor 488 conjugated anti-mouse antibody (Life Technologies, Rockville, MD) at 1:400 dilution in blocking buffer for 1 hour at room temperature. Nuclei were stained with 4′,6-diamidino-2-phenylindole in blocking buffer. Imaging and quantification of relative intensities of fluorescence signals were performed with the Cytation 5 multimode reader and Gen5 software (BioTek).

Targeted Mass Spectrometry

Samples were resuspended using 20 μL high-performance liquid chromatography (HPLC) grade water for MS; 5 μL were injected and analyzed by using a hybrid 5500 QTRAP triple quadrupole mass spectrometer (AB/Sciex, Redwood City, CA) coupled to a Prominence UFLC HPLC system (Shimadzu, Kyoto, Japan) via selected reaction monitoring (SRM) of a total of 256 endogenous water-soluble metabolites for steady-state analyses of sample.[13] Some metabolites were targeted in both positive and negative ion mode for a total of 289 SRM transitions using positive/negative ion polarity switching. ESI voltage was +4900 V in positive ion mode and –4500 V in negative ion mode. The dwell time was 3 ms per SRM transition, and the total cycle time was 1.55 seconds. Approximately 10–14 data points were acquired per detected metabolite. Samples were delivered to the mass spectrometer via hydrophilic interaction chromatography by using a 4.6-mm inner diameter × 10 cm Amide XBridge column (Waters Corp, Milford, MA) at 400 μL/min. Gradients were run starting from 85% buffer B (HPLC grade acetonitrile) to 42% B from 0 to 5 minutes; 42% B to 0% B from 5 to 16 minutes; 0% B was held from 16 to 24 minutes; 0% B to 85% B from 24 to 25 minutes; and 85% B was held for 7 minutes to re-equilibrate the column. Buffer A was composed of 20 mmol/L ammonium hydroxide/20 mmol/L ammonium acetate (pH 9.0) in 95:5 water:acetonitrile. Peak areas from the total ion current for each metabolite SRM transition were integrated using MultiQuant, version 2.0, software (AB/Sciex).

Metabolite Profile Analyses

Relative intensities of metabolites were normalized to cell number. Metabolite Set Enrichment Analysis (MSEA) was performed on the MetaboAnalyst Web server with lists of metabolites with fold change of more than or equal to 1.3 either up or down in the isogenic SALL4 expression cell lines compared with empty vector control, with Student 2-tailed t test P value of <.05.[14]

L-Lactate Cellular Measurements

The L-lactate Assay kit (Abcam) was used to measure cellular lactate levels. First, 2.2 × 10^6 cells were washed in ice-cold PBS twice, then they were lysed in 220 μL of assay buffer to achieve a concentration of 10,000 cells/μL. Lysates were then spun down at 13,000 rpm for 5 minutes at 4°C to pellet insoluble debris. Soluble fractions were then filtered through >30-kDa centrifugal filter units (Amicon) (Merck Millipore, Burlington, MA) and spun at 14,000 rpm for 20 minutes at 4°C to remove endogenous lactate dehydrogenase subunits (35 kDa) from the lysates. The assay was then performed according to the manufacturer's protocol with 50 μL of lysate (500,000 cells) per well in a 96-well plate and the inclusion of L-lactate standards to plot a standard curve for lactate quantification.

Oxygen Consumption Rate and Glycolysis Stress Test Measurements

Cells were harvested and plated in the Seahorse XFe96 96-well miniplates (Agilent) coated with collagen. Cell numbers plated were 15,000 for the SNU-387, SNU-387 empty vector, and *Tg:SALL4A* and *Tg:SALL4B* cell lines; 25,000 for the SNU-398 and SNU-398 sh-scr cell lines; 35,000 for the SNU-398 shSALL4-1 knockdown cell line; and 40,000 for the SNU-398 shSALL4-2 knockdown cell line. After overnight incubation, cells were washed and medium was replaced with the recommended Seahorse Mitostress DMEM media and placed in a CO_2-free 37°C incubator for 1 hour. Basal oxygen consumption was then measured by the Seahorse XFe96 Analyzer (Agilent) according to the manufacturer's recommended protocol. The glycolysis stress test was also performed on the isogenic SALL4-expressing cell lines, prepared as described earlier, according to the manufacturer's recommended protocol. Cells were also subjected to the CyQUANT DNA quantification assay (Thermo Fisher Scientific) to measure DNA content, serving as a basis to normalize oxygen consumption rates with respect to cell number.

RNA/DNA Extraction and Quantitative Reverse-Transcription Polymerase Chain Reaction Analysis

RNA isolation was performed using the RNeasy Plus Mini Kit (Qiagen). Genomic/mitochondrial DNA isolation was performed using the QIAamp DNA Mini Kit (Qiagen). cDNA was synthesized from purified RNA with the High Capacity cDNA Reverse Transcription Kit (Applied Biosystems, Foster City, CA). Quantitative PCR for cDNA or genomic/mitochondrial DNA was performed on the ViiA 7 Real-Time PCR system (Thermo Fisher Scientific) with the PowerUP SYBR Green Master Mix (Applied Biosystems). The ΔΔcycle threshold method was used for relative quantification. RT-PCR primers are as follows:

18S rRNA forward: 5′-GTAACCCGTTGAACCCCATT-3′

18S rRNA reverse: 5′-CCATCCAATCGGTAGTAGCG-3′

ACTB forward: 5′-CAGAGCCTCGCCTTTGCCGATC-3′

ACTB reverse: 5′-CATCCATGGTGAGCTGGCGGCG-3′

ARG2 forward: 5′-CGCGAGTGCATTCCATCCT-3′

ARG2 reverse: 5′-TCCAAAGTCTTTTAGGTGGCAG-3′

B2M forward: 5′-CACTGAAAAAGATGAGTATGCC-3′

B2M reverse: 5′-AACATTCCCTGACAATCCC-3′

CLYBL forward: 5′-TCCCCAGACTTGGATATAGTTCC-3′

CLYBL reverse: 5′-TGCACAATCTACATTCAGGGATG-3′

MinorArc forward: 5′-CTAAATAGCCCACACGTTCCC-3′

MinorArc reverse: 5′-AGAGCTCCCGTGAGTGGTTA-3′

MRPL24 forward: 5′-GCCAGGTCAAACTTGTGGAT-3′

MRPL24 reverse: 5′-CCCTGATCGTGTGGAGACTC-3′

ND1 forward: 5′-ACGCCATAAAACTCTTCACCAAAG-3′

ND1 reverse: 5′-GGGTTCATAGTAGAAGAGCGATGG-3′

ND4 forward: 5′-ACCTTGGCTATCATCACCCGAT-3′

ND4 reverse: 5′-AGTGCGATGAGTAGGGGAAGG-3′

NRF1 forward: 5′-AGGAACACGGAGTGACCCAA-3′

NRF1 reverse: 5′-TGCATGTGCTTCTATGGTAGC-3′

NRF2 forward: 5′-AAGTGACAAGATGGGCTGCT-3′

NRF2 reverse: 5′-TGGACCACTGTATGGGATCA-3′

PGC-1α forward: 5′-CAAGCCAAACCAACAACTTTATCTCT-3′

PGC-1α reverse: 5′-CACACTTAAGGTGCGTTCAATAGTC-3′

PGC-1β forward: 5′-GGCAGGTTCAACCCCGA-3′

PGC-1β reverse: 5′-CTTGCTAACATCACAGAGGA-TATCTTG-3′

SALL4 forward: 5′-GCGAGCTTTTACCACCAAAG-3′

SALL4 reverse: 5′-CACAACAGGGTCCACATTCA-3′

SALL4A forward: 5′-TCCCCAGACTTGGATATAGTTCC-3′

SALL4A reverse: 5′-TGCACAATCTACATTCAGGGATG-3′

SALL4B forward: 5′-GGTGGATGTCAAACCCAAAG-3′

SALL4B reverse: 5′-ATGTGCCAGGAACTTCAACC-3′

SLC25A10 forward: 5′-GTGTCGCGCTGGTACTTC-3′

SLC25A10 reverse: 5′-CACCTCCTGCTGCGTCTG-3′

SUMO1 forward: 5′-TTGGAACACCCTGTCTTTGAC-3′

SUMO1 reverse: 5′-ACCGTCATCATGTCTGACCA-3′

TFAM forward: 5′-CCGAGGTGGTTTTCATCTGT-3′

TFAM reverse: 5′-ACGCTGGGCAATTCTTCTAA-3′

Supplementary References

1. Butler MS, Yoganathan K, Buss AD, et al. Identification of aluminium dioxalate in fungal cultures grown on vermiculite. J Antibiot (Tokyo) 2012;65:275–276.
2. Boot CM, Tenney K, Valeriote FA, et al. Highly *N*-methylated linear peptides produced by an atypical sponge-derived *Acremonium* sp. J Nat Prod 2006;69: 83–92.
3. Yong KJ, Gao C, Lim JSJ, et al. Oncofetal gene *SALL4* in aggressive hepatocellular carcinoma. N Engl J Med 2013;368:2266–2276.
4. **Liu BH, Jobichen C**, Chia CSB, et al. Targeting cancer addiction for SALL4 by shifting its transcriptome with a pharmacologic peptide. Proc Natl Acad Sci U S A 2018; 115:E7119–E7128.
5. **Li H, Handsaker B**, Wysoker A, et al. The Sequence Alignment/Map format and SAMtools. Bioinformatics 2009;25:2078–2079.

6. Heinz S, Benner C, Spann N, et al. Simple combinations of lineage-determining transcription factors prime cis-regulatory elements required for macrophage and B Cell identities. Mol Cell 2010;38:576–589.
7. Quinlan AR, Hall IM. BEDTools: a flexible suite of utilities for comparing genomic features. Bioinformatics 2010; 26:841–842.
8. **Ramírez F, Ryan DP**, Grüning B, et al. deepTools2: a next generation web server for deep-sequencing data analysis. Nucleic Acids Res 2016;44:W160–W165.
9. Li A, Jiao Y, Yong KJ, et al. SALL4 is a new target in endometrial cancer. Oncogene 2015;34:63–72.
10. Kim D, Pertea G, Trapnell C, et al. TopHat2: accurate alignment of transcriptomes in the presence of insertions, deletions and gene fusions. Genome Biol 2013;14:R36.
11. Trapnell C, Roberts A, Goff L, et al. Differential gene and transcript expression analysis of RNA-seq experiments with TopHat and Cufflinks. Nat Protoc 2012;7:562–578.
12. **Subramanian A, Tamayo P**, Mootha VK, et al. Gene set enrichment analysis: a knowledge-based approach for interpreting genome-wide expression profiles. Proc Natl Acad Sci U S A 2005;102:15545–15550.
13. **Yuan M, Breitkopf SB**, Yang X, et al. A positive/negative ion-switching, targeted mass spectrometry-based metabolomics platform for bodily fluids, cells, and fresh and fixed tissue. Nat Protoc 2012;7:872–881.
14. Xia J, Wishart DS. MSEA: a web-based tool to identify biologically meaningful patterns in quantitative metabolomic data. Nucleic Acids Res 2010;38:W71–W77.

Author names in bold designate shared co-first authorship.

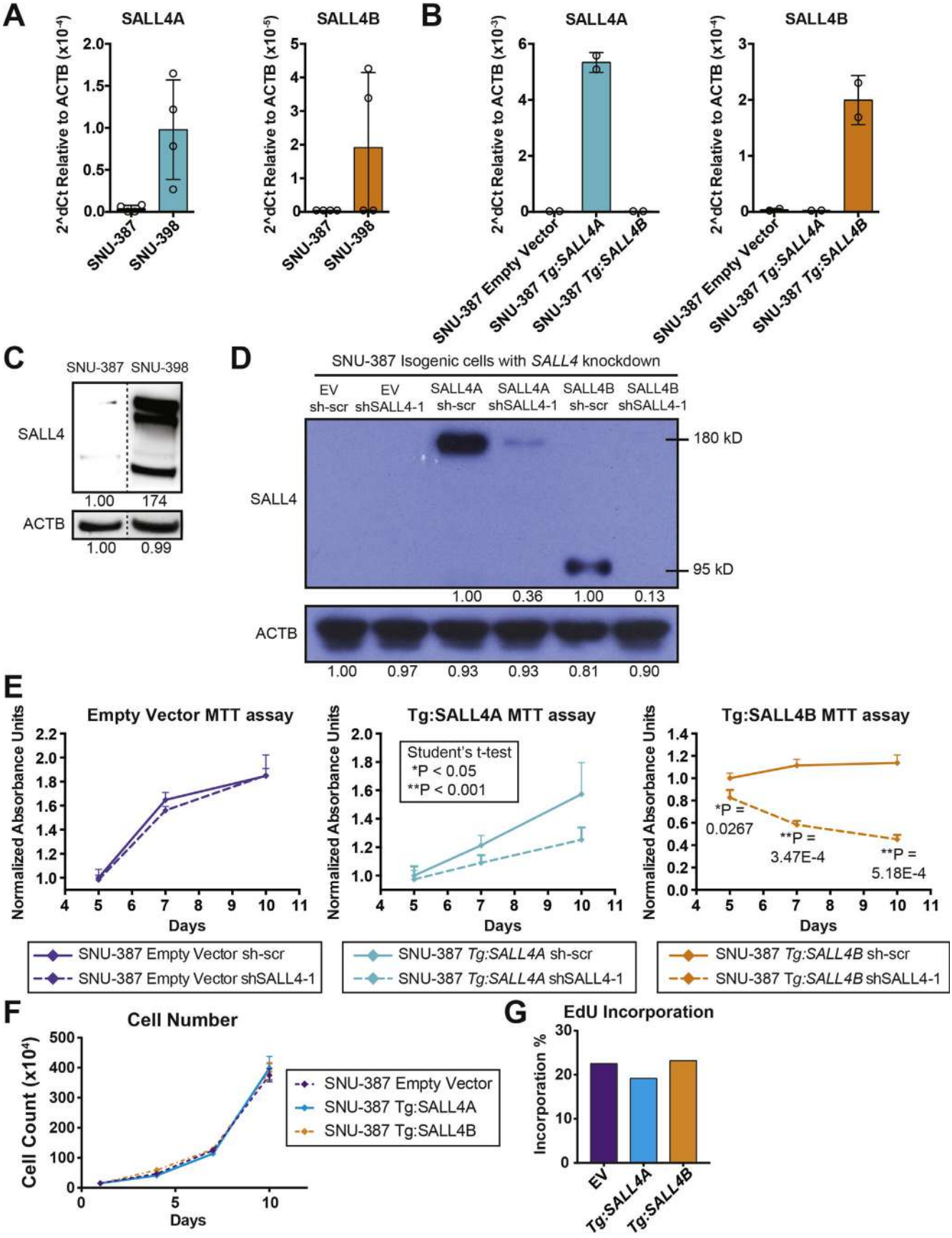
A
SALL4A
2^dCt Relative to ACTB (x10⁻⁴)
SNU-387
SNU-398
SALL4B
2^dCt Relative to ACTB (x10⁻⁵)
B
SALL4A
2^dCt Relative to ACTB (x10⁻³)
SNU-387 Empty Vector
SNU-387 Tg:SALL4A
SNU-387 Tg:SALL4B
SALL4B
2^dCt Relative to ACTB (x10⁻⁴)
C
SNU-387 SNU-398
SALL4
1.00 174
ACTB
1.00 0.99
D
SNU-387 Isogenic cells with SALL4 knockdown
EV sh-scr
EV shSALL4-1
SALL4A sh-scr
SALL4A shSALL4-1
SALL4B sh-scr
SALL4B shSALL4-1
SALL4
180 kD
95 kD
1.00 0.36 1.00 0.13
ACTB
1.00 0.97 0.93 0.93 0.81 0.90
E
Empty Vector MTT assay
Tg:SALL4A MTT assay
Student's t-test
*P < 0.05
**P < 0.001
Tg:SALL4B MTT assay
*P = 0.0267
**P = 3.47E-4
**P = 5.18E-4
Normalized Absorbance Units
Days
SNU-387 Empty Vector sh-scr
SNU-387 Empty Vector shSALL4-1
SNU-387 Tg:SALL4A sh-scr
SNU-387 Tg:SALL4A shSALL4-1
SNU-387 Tg:SALL4B sh-scr
SNU-387 Tg:SALL4B shSALL4-1
F
Cell Number
Cell Count (x10⁴)
Days
SNU-387 Empty Vector
SNU-387 Tg:SALL4A
SNU-387 Tg:SALL4B
G
EdU Incorporation
Incorporation %
EV
Tg:SALL4A
Tg:SALL4B

Supplementary Figure 1. SALL4 isogenic cell lines are dependent on SALL4 for cell viability. (*A*) *SALL4* mRNA expression in *SALL4* endogenous cell lines used in the screening, measured by qRT-PCR and normalized to *ACTB* (mean of 4 replicates ± SD). (*B*) *SALL4* mRNA expression in SNU-387 isogenic empty vector and *SALL4A*- and *SALL4B*-expressing cell lines used in the screen, measured by qRT-PCR and normalized to *ACTB* (mean of 2 replicates ± SD). (*C*) Western blot of SALL4 protein in the *SALL4* endogenous cell lines, with ACTB loading control. Bands were quantified by densitometry with SNU-387 bands as reference. (*D*) Western blot of SALL4 protein isoforms and *SALL4* knockdown validation in the isogenic cell lines, with ACTB loading control. Bands were quantified by densitometry with sh-scr bands as reference. (*E*) MTT oxidoreductase-dependent cell viability assay on *SALL4* isogenic cell lines with *SALL4* knockdown, normalized to day 5 sh-scr scrambled control (mean of 3 replicates ± SD). (*F*) Cell counts of SALL4-expressing isogenic cell lines over 10 days (mean of 3 replicates ± SD). (*G*) EdU incorporation, during DNA synthesis, of measurements for the percentage of EdU-labeled cells after 3 hours of treatment for the SALL4-expressing isogenic cell lines (performed in singlet). EV, empty vector; SD, standard deviation.

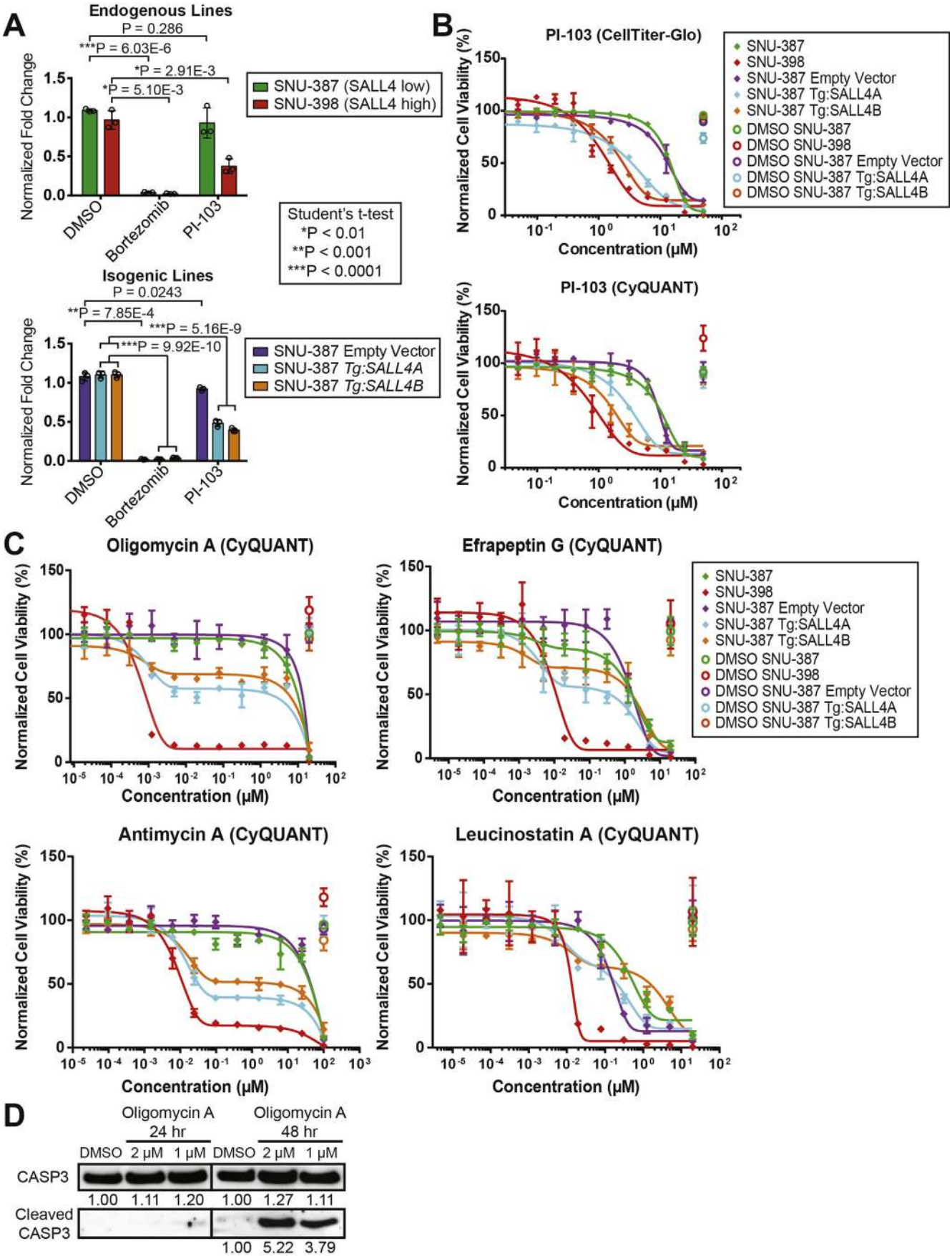
A
Endogenous Lines
P = 0.286
***P = 6.03E-6
*P = 2.91E-3
*P = 5.10E-3
Normalized Fold Change
SNU-387 (SALL4 low)
SNU-398 (SALL4 high)
DMSO
Bortezomib
PI-103
Student's t-test
*P < 0.01
**P < 0.001
***P < 0.0001
Isogenic Lines
P = 0.0243
**P = 7.85E-4
***P = 5.16E-9
***P = 9.92E-10
SNU-387 Empty Vector
SNU-387 Tg:SALL4A
SNU-387 Tg:SALL4B
B
PI-103 (CellTiter-Glo)
Normalized Cell Viability (%)
Concentration (μM)
SNU-387
SNU-398
SNU-387 Empty Vector
SNU-387 Tg:SALL4A
SNU-387 Tg:SALL4B
DMSO SNU-387
DMSO SNU-398
DMSO SNU-387 Empty Vector
DMSO SNU-387 Tg:SALL4A
DMSO SNU-387 Tg:SALL4B
PI-103 (CyQUANT)
C
Oligomycin A (CyQUANT)
Efrapeptin G (CyQUANT)
Antimycin A (CyQUANT)
Leucinostatin A (CyQUANT)
D
Oligomycin A
24 hr
48 hr
DMSO 2 μM 1 μM DMSO 2 μM 1 μM
CASP3
1.00 1.11 1.20 1.00 1.27 1.11
Cleaved CASP3
1.00 5.22 3.79

Supplementary Figure 2. Natural product and small molecule screening hits. (*A*) Cell viability fold change plots of control compounds obtained from the pilot screening and used for the complete screening, measured with CellTiter-Glo cell viability reagent and normalized to DMSO-treated cell viability (mean of 3 replicates ± SD). (*B*) Cell viability dose response curves for cells treated for 96 hours with synthetic compound hit PI-103, measured with CellTiter-Glo and CyQUANT reagents and normalized to untreated cell viability (mean of 3 replicates ± SD). (*C*) Cell viability dose response curves for cells treated for 96 hours with hit compounds from the natural product extract screening (oligomycin, efrapeptin, antimycin, and leucinostatin), measured with CyQUANT reagent and normalized to untreated cell viability (mean of 3 replicates ± SD). (*D*) Western blot for apoptosis marker cleaved caspase-3 and control total caspase-3 protein levels in oligomycin A-treated SNU-398 cells. Bands were quantified by densitometry with DMSO bands as reference. M, mol/L; SD, standard deviation.

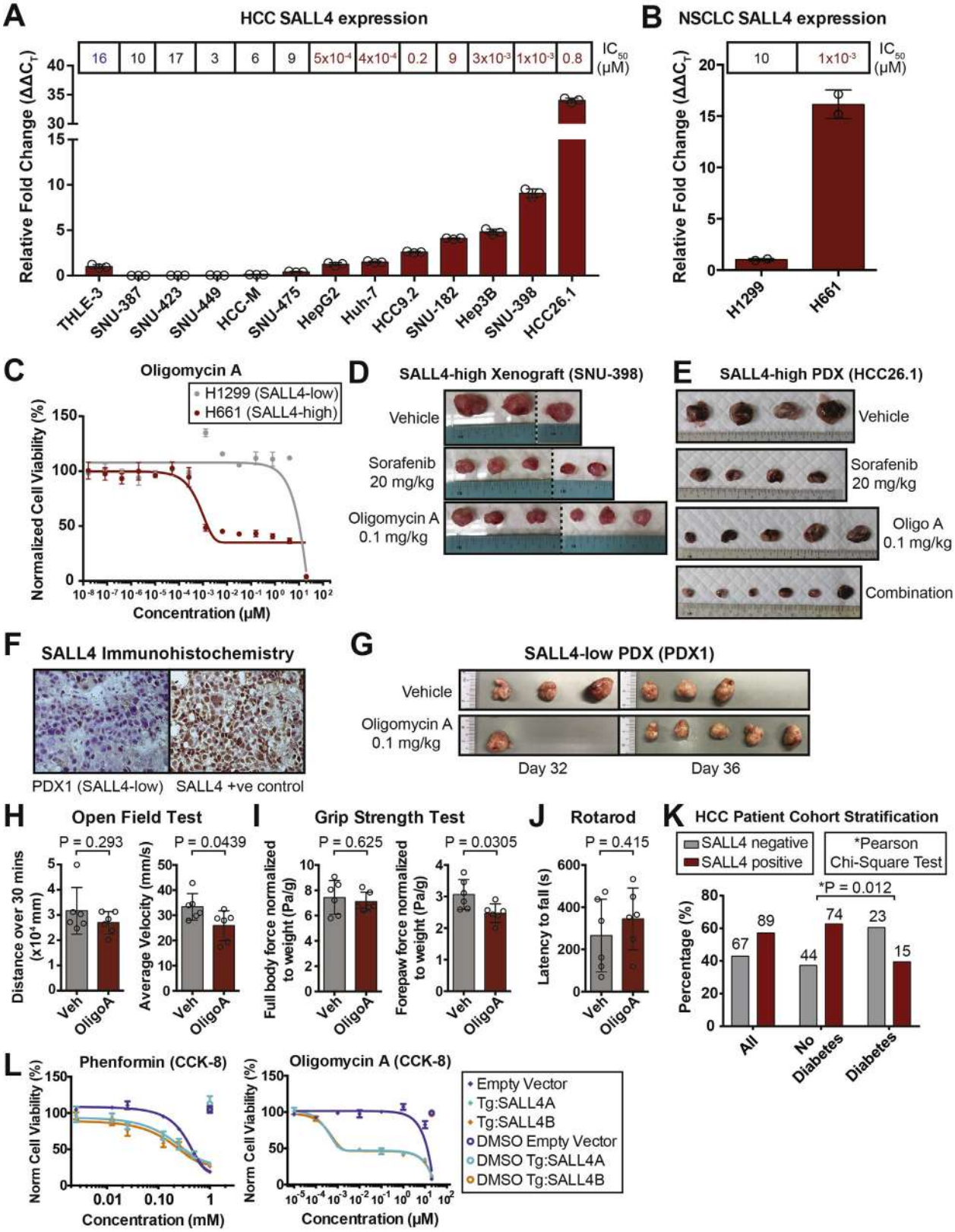
A
HCC SALL4 expression
IC50 (μM)
16
10
17
3
6
9
5x10-4
4x10-4
0.2
9
3x10-3
1x10-3
0.8
Relative Fold Change (ΔΔCT)
THLE-3
SNU-387
SNU-423
SNU-449
HCC-M
SNU-475
HepG2
Huh-7
HCC9.2
SNU-182
Hep3B
SNU-398
HCC26.1
B
NSCLC SALL4 expression
10
1x10-3
H1299
H661
C
Oligomycin A
H1299 (SALL4-low)
H661 (SALL4-high)
Normalized Cell Viability (%)
Concentration (μM)
D
SALL4-high Xenograft (SNU-398)
Vehicle
Sorafenib 20 mg/kg
Oligomycin A 0.1 mg/kg
E
SALL4-high PDX (HCC26.1)
Vehicle
Sorafenib 20 mg/kg
Oligo A 0.1 mg/kg
Combination
F
SALL4 Immunohistochemistry
PDX1 (SALL4-low)
SALL4 +ve control
G
SALL4-low PDX (PDX1)
Vehicle
Oligomycin A 0.1 mg/kg
Day 32
Day 36
H
Open Field Test
P = 0.293
P = 0.0439
Distance over 30 mins (x10⁴ mm)
Average Velocity (mm/s)
Veh
OligoA
I
Grip Strength Test
P = 0.625
P = 0.0305
Full body force normalized to weight (Pa/g)
Forepaw force normalized to weight (Pa/g)
J
Rotarod
P = 0.415
Latency to fall (s)
K
HCC Patient Cohort Stratification
SALL4 negative
SALL4 positive
*Pearson Chi-Square Test
*P = 0.012
Percentage (%)
67
89
44
74
23
15
All
No Diabetes
Diabetes
L
Phenformin (CCK-8)
Oligomycin A (CCK-8)
Norm Cell Viability (%)
Concentration (mM)
Concentration (μM)
Empty Vector
Tg:SALL4A
Tg:SALL4B
DMSO Empty Vector
DMSO Tg:SALL4A
DMSO Tg:SALL4B

Supplementary Figure 3. Oligomycin A suppresses SALL4-dependent tumorigenesis. (*A*) *SALL4* mRNA expression in HCC cell lines with respect to immortalized normal liver cell line THLE-3 *SALL4* transcript levels, measured by qRT-PCR and normalized to *18S* ribosomal RNA (mean of 3 replicates ± SD). Oligomycin A IC_{50} values from dose response curves in Figure 3*A* are detailed above the bar graphs for corresponding cell lines. (*B*) *SALL4* mRNA expression in a pair of $SALL4^{hi}$ and $SALL4^{lo}$ NSCLC cell lines with respect to immortalized normal liver cell line THLE-3 *SALL4* transcript levels, measured by qRT-PCR and normalized to *18S* rRNA (mean of 2 replicates ± SD). Oligomycin A IC_{50} values from dose response curves in *C* are detailed above the bar graphs for corresponding cell lines. (*C*) Cell viability dose response curves for lung cancer cell lines in (*B*) treated with oligomycin A, measured with CellTiter-Glo reagent and normalized to untreated cell viability (mean of 3 replicates ± SD). (*D*) Tumor images from the SNU-398 mouse xenograft experiment in Figure 3*B*. (*D*) Tumor images from the SNU-398 mouse xenograft experiment in Figure 3*C*. (*E*) Tumor images from the HCC26.1 mouse patient-derived xenograft experiment in Figure 3*E*. (*F*) SALL4 immunohistochemistry on a PDX1 tumor section and a SALL4-positive control tumor section. (*G*) Tumor images from the PDX1 mouse patient-derived xenograft experiment in Figure 3*G*. Four tumors were excised on day 32 as their size reached the designated animal protocol endpoint while the remaining mice continued drug treatment until day 36, when all remaining tumors reached the endpoint. (*H*) Open field test conducted on mice injected with vehicle (n = 6) and 0.1 mg/kg oligomycin A (n = 6) over 3 weeks (mean ± SD). (*I*) Grip strength test conducted on the mice in *H* (mean ± SD). (*J*) Rotarod test conducted on the mice in *H* (mean ± SD). (*K*) HCC patient stratification by SALL4 expression and diabetics. Numbers above bar graphs indicate absolute patient numbers. (*L*) Cell viability dose response curves for cells treated for 96 hours with phenformin or oligomycin A, measured with Cell Counting Kin-8 dehydrogenase activity assay and normalized to untreated cell viability (mean of 3 replicates ± SD). SD, standard deviation.

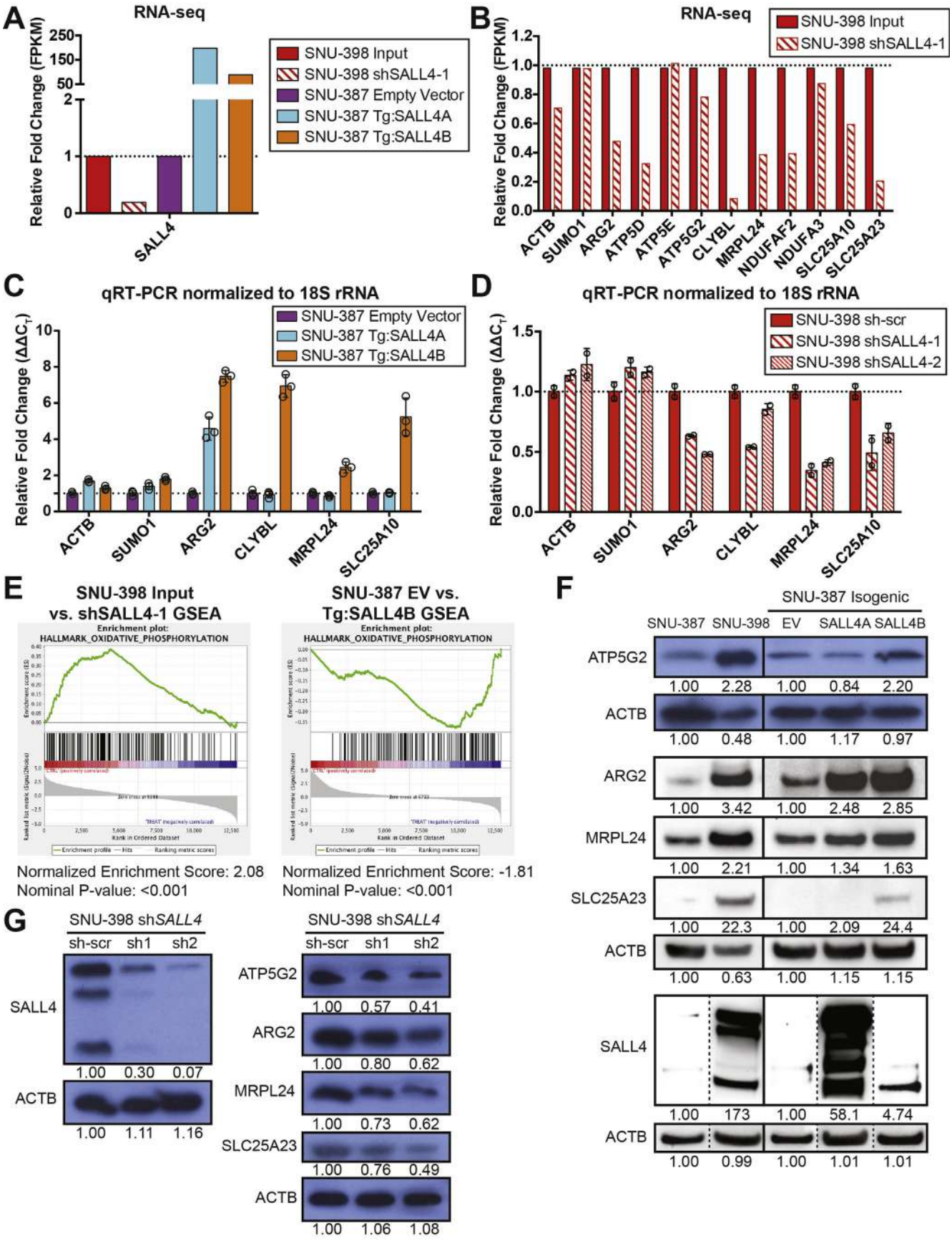
A
RNA-seq
Relative Fold Change (FPKM)
SNU-398 Input
SNU-398 shSALL4-1
SNU-387 Empty Vector
SNU-387 Tg:SALL4A
SNU-387 Tg:SALL4B
SALL4
B
RNA-seq
Relative Fold Change (FPKM)
SNU-398 Input
SNU-398 shSALL4-1
ACTB
SUMO1
ARG2
ATP5D
ATP5E
ATP5G2
CLYBL
MRPL24
NDUFAF2
NDUFA3
SLC25A10
SLC25A23
C
qRT-PCR normalized to 18S rRNA
Relative Fold Change (ΔΔCT)
SNU-387 Empty Vector
SNU-387 Tg:SALL4A
SNU-387 Tg:SALL4B
ACTB
SUMO1
ARG2
CLYBL
MRPL24
SLC25A10
D
qRT-PCR normalized to 18S rRNA
Relative Fold Change (ΔΔCT)
SNU-398 sh-scr
SNU-398 shSALL4-1
SNU-398 shSALL4-2
ACTB
SUMO1
ARG2
CLYBL
MRPL24
SLC25A10
E
SNU-398 Input vs. shSALL4-1 GSEA
Enrichment plot:
HALLMARK_OXIDATIVE_PHOSPHORYLATION
Normalized Enrichment Score: 2.08
Nominal P-value: <0.001
SNU-387 EV vs. Tg:SALL4B GSEA
Enrichment plot:
HALLMARK_OXIDATIVE_PHOSPHORYLATION
Normalized Enrichment Score: -1.81
Nominal P-value: <0.001
F
SNU-387 Isogenic
SNU-387 SNU-398 EV SALL4A SALL4B
ATP5G2
1.00 2.28 1.00 0.84 2.20
ACTB
1.00 0.48 1.00 1.17 0.97
ARG2
1.00 3.42 1.00 2.48 2.85
MRPL24
1.00 2.21 1.00 1.34 1.63
SLC25A23
1.00 22.3 1.00 2.09 24.4
ACTB
1.00 0.63 1.00 1.15 1.15
SALL4
1.00 173 1.00 58.1 4.74
ACTB
1.00 0.99 1.00 1.01 1.01
G
SNU-398 shSALL4
sh-scr sh1 sh2
SALL4
1.00 0.30 0.07
ACTB
1.00 1.11 1.16
SNU-398 shSALL4
sh-scr sh1 sh2
ATP5G2
1.00 0.57 0.41
ARG2
1.00 0.80 0.62
MRPL24
1.00 0.73 0.62
SLC25A23
1.00 0.76 0.49
ACTB
1.00 1.06 1.08

Supplementary Figure 4. SALL4 expression up-regulates oxidative phosphorylation gene expression. (*A*) RNA-seq expression level fold change for SALL4, in the SNU-398 *SALL4*-knockdown and isogenic *SALL4*-expressing cell lines, normalized respectively to expression levels in the SNU-398 input and SNU-387 empty vector control cell line, performed in singlet. (*B*) RNA-seq expression level fold change for a panel of mitochondrial genes from Figure 4*D* with *SALL4* knockdown in the SNU-398 cells, normalized to expression levels in the SNU-398 control, performed in singlet. (*C*) mRNA expression validation of selected mitochondrial genes in the *SALL4*-expressing isogenic cell lines used in the screening, measured by qRT-PCR and normalized to *18S* ribosomal RNA (mean of 3 replicates ± SD). (*D*) mRNA expression validation of the mitochondrial genes from *C* with *SALL4* knockdown for 72 hours in the SNU-398 cell line, measured by qRT-PCR and normalized to *18S* ribosomal RNA (mean of 2 replicates ± SD). (*E*) GSEA plots for oxidative phosphorylation from analysis of the RNA-seq data set in *A*. (*F*) Western blots for SALL4-bound mitochondrial genes and ACTB loading control in the cell lines used in the screening. Bands were quantified by densitometry with SNU-387 and EV bands as references. (*G*) Western blots for the genes in *F* in the SNU-398 cell line 72 hours after *SALL4* knockdown. Bands were quantified by densitometry with sh-scr bands as reference. EV, empty vector; SD, standard deviation.

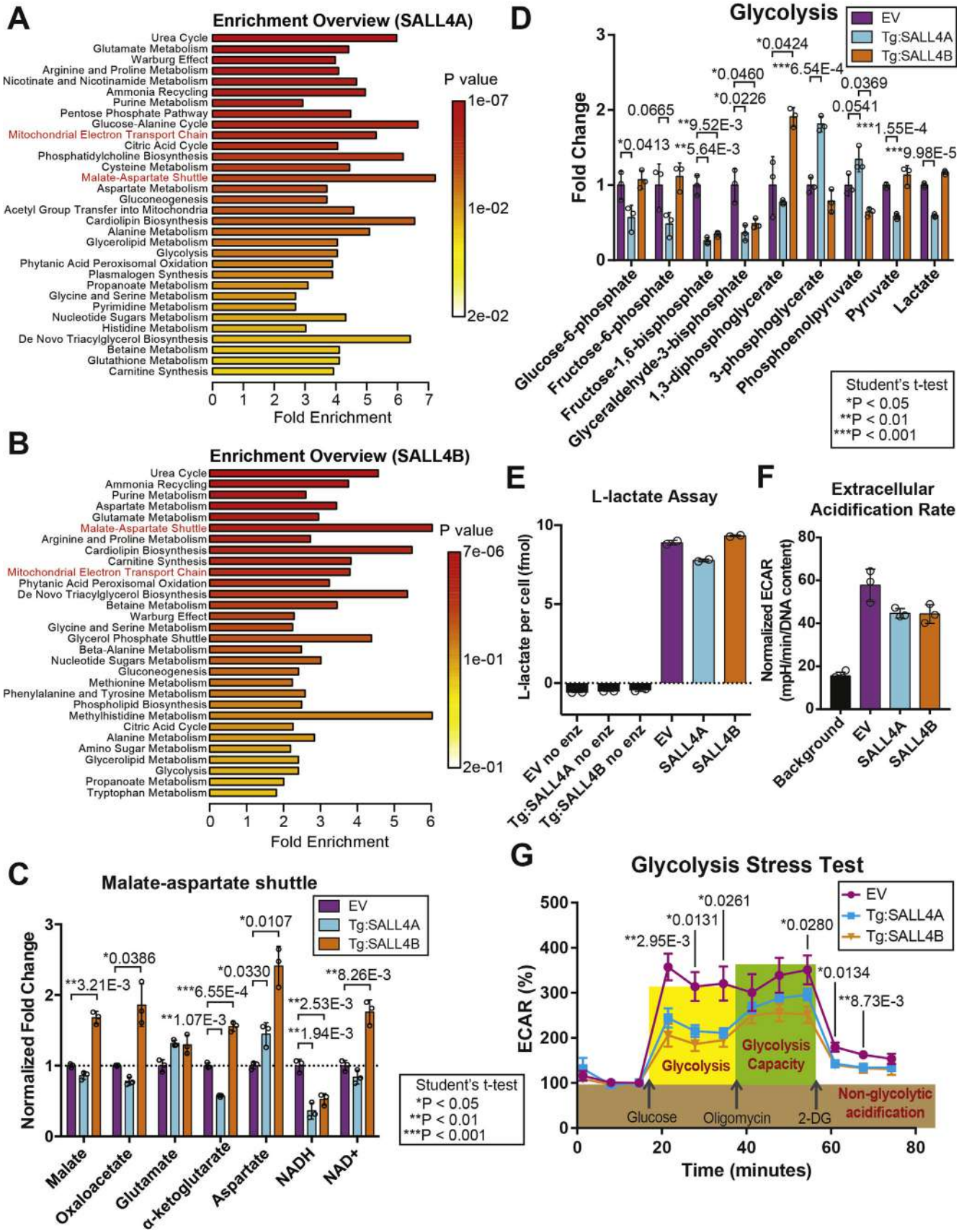
A
Enrichment Overview (SALL4A)
Urea Cycle
Glutamate Metabolism
Warburg Effect
Arginine and Proline Metabolism
Nicotinate and Nicotinamide Metabolism
Ammonia Recycling
Purine Metabolism
Pentose Phosphate Pathway
Glucose-Alanine Cycle
Mitochondrial Electron Transport Chain
Citric Acid Cycle
Phosphatidylcholine Biosynthesis
Cysteine Metabolism
Malate-Aspartate Shuttle
Aspartate Metabolism
Gluconeogenesis
Acetyl Group Transfer into Mitochondria
Cardiolipin Biosynthesis
Alanine Metabolism
Glycerolipid Metabolism
Glycolysis
Phytanic Acid Peroxisomal Oxidation
Plasmalogen Synthesis
Propanoate Metabolism
Glycine and Serine Metabolism
Pyrimidine Metabolism
Nucleotide Sugars Metabolism
Histidine Metabolism
De Novo Triacylglycerol Biosynthesis
Betaine Metabolism
Glutathione Metabolism
Carnitine Synthesis
P value
1e-07
1e-02
2e-02
0 1 2 3 4 5 6 7
Fold Enrichment
B
Enrichment Overview (SALL4B)
Urea Cycle
Ammonia Recycling
Purine Metabolism
Aspartate Metabolism
Glutamate Metabolism
Malate-Aspartate Shuttle
Arginine and Proline Metabolism
Cardiolipin Biosynthesis
Carnitine Synthesis
Mitochondrial Electron Transport Chain
Phytanic Acid Peroxisomal Oxidation
De Novo Triacylglycerol Biosynthesis
Betaine Metabolism
Warburg Effect
Glycine and Serine Metabolism
Glycerol Phosphate Shuttle
Beta-Alanine Metabolism
Nucleotide Sugars Metabolism
Gluconeogenesis
Methionine Metabolism
Phenylalanine and Tyrosine Metabolism
Phospholipid Biosynthesis
Methylhistidine Metabolism
Citric Acid Cycle
Alanine Metabolism
Amino Sugar Metabolism
Glycerolipid Metabolism
Glycolysis
Propanoate Metabolism
Tryptophan Metabolism
P value
7e-06
1e-01
2e-01
0 1 2 3 4 5 6
Fold Enrichment
C
Malate-aspartate shuttle
EV
Tg:SALL4A
Tg:SALL4B
Normalized Fold Change
**3.21E-3
*0.0386
**1.07E-3
***6.55E-4
*0.0330
*0.0107
**1.94E-3
**2.53E-3
**8.26E-3
Malate
Oxaloacetate
Glutamate
α-ketoglutarate
Aspartate
NADH
NAD+
Student's t-test
*P < 0.05
**P < 0.01
***P < 0.001
D
Glycolysis
EV
Tg:SALL4A
Tg:SALL4B
Fold Change
*0.0413
0.0665
**5.64E-3
**9.52E-3
*0.0460
*0.0226
*0.0424
***6.54E-4
0.0369
0.0541
***1.55E-4
***9.98E-5
Glucose-6-phosphate
Fructose-6-phosphate
Fructose-1,6-bisphosphate
Glyceraldehyde-3-bisphosphate
1,3-diphosphoglycerate
3-phosphoglycerate
Phosphoenolpyruvate
Pyruvate
Lactate
Student's t-test
*P < 0.05
**P < 0.01
***P < 0.001
E
L-lactate Assay
L-lactate per cell (fmol)
EV no enz
Tg:SALL4A no enz
Tg:SALL4B no enz
EV
SALL4A
SALL4B
F
Extracellular Acidification Rate
Normalized ECAR (mpH/min/DNA content)
Background
EV
SALL4A
SALL4B
G
Glycolysis Stress Test
EV
Tg:SALL4A
Tg:SALL4B
ECAR (%)
**2.95E-3
*0.0131
*0.0261
*0.0280
*0.0134
**8.73E-3
Glycolysis
Glycolysis Capacity
Non-glycolytic acidification
Glucose
Oligomycin
2-DG
Time (minutes)

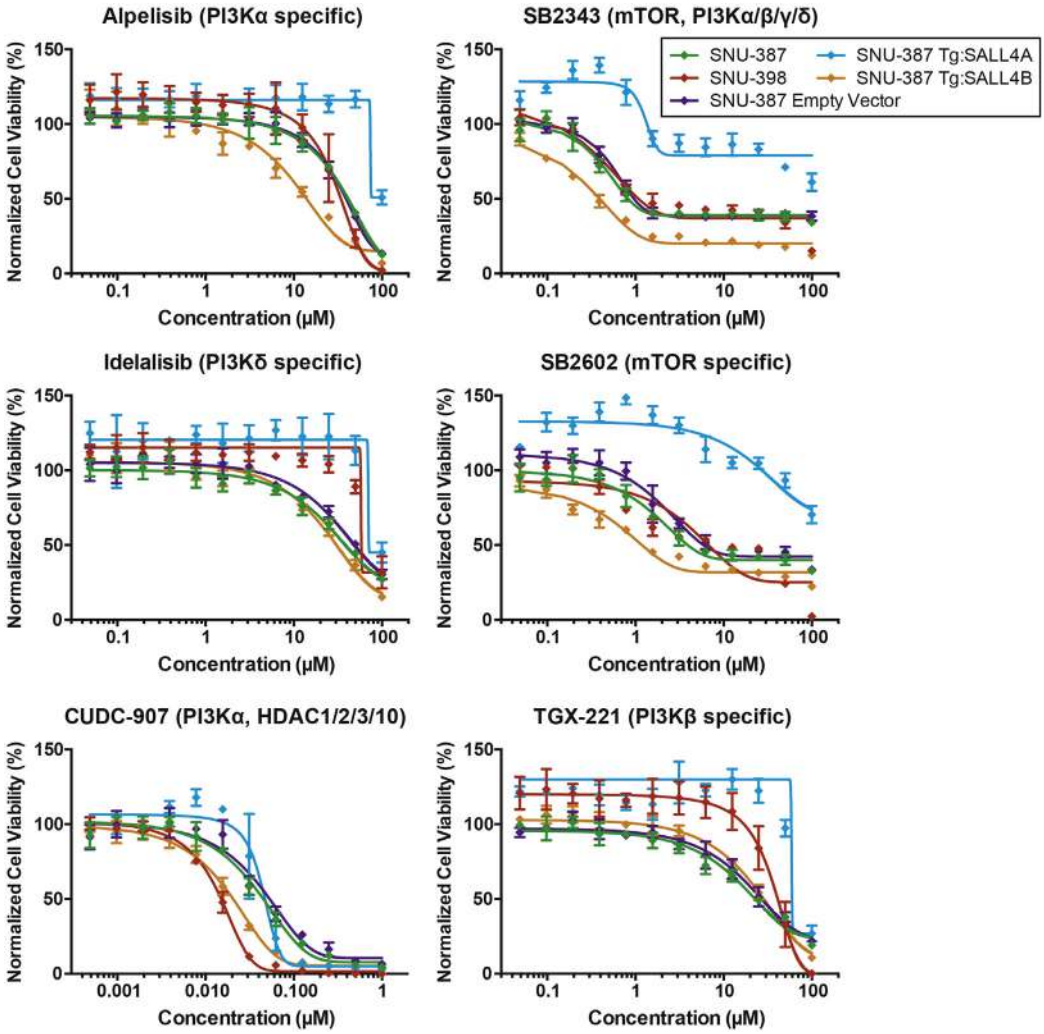

Supplementary Figure 6. PI3K and mTOR inhibitor have limited selectivity for SALL4-expressing cells. Cell viability dose response curves for cells treated for 72 hours with selective PI3K or mTOR inhibitors alpelisib, SB2343, idelalisib, SB2602, CUDC-907, and TGX-221 measured with CellTiter-Glo reagent and normalized to DMSO-treated cell viability (mean of 3 replicates ± SD). M, mol/L; SD, standard deviation.

Supplementary Figure 5. Oxidative phosphorylation and glycolysis metabolite changes induced by SALL expression. (*A*) Metabolite Set Enrichment Analysis of significantly altered metabolites (1.3-fold change, $P < .05$) in the SNU-387 *Tg:SALL4A* cells compared with empty vector control. (*B*) Metabolite Set Enrichment Analysis of significantly altered metabolites (1.3-fold change, $P < .05$) in the SNU-387 *Tg:SALL4B* cells compared with empty vector control. (*C*) Fold change of malate-aspartate shuttle metabolites in the SALL4-expressing isogenic lines normalized to empty vector control (mean of 3 replicates ± SD). (*D*) Fold change of glycolytic metabolites in the SALL4-expressing isogenic lines normalized to empty vector control (mean of 3 replicates ± SD). (*E*) L-lactate measurements, using a lactate dehydrogenase enzymatic assay, in the SALL4 isogenic cell lines and no enzyme controls, normalized by cell number (mean of 2 replicates ± SD). (*F*) Extracellular acidification rate (ECAR) measurements per DNA content in the SALL4 isogenic lines, normalized to CyQUANT DNA quantification reagent values (mean of 3 replicates ± SD). (*G*) Glycolysis stress test assessing ECAR when cells are treated with glucose after starvation, ATP synthase inhibitor oligomycin, and glycolysis inhibitor 2-deoxy-D-glucose that quantifies glycolytic flux and glycolytic capacity, performed on the SALL4-expressing isogenic lines (mean of 3 replicates ± SD). SD, standard deviation.

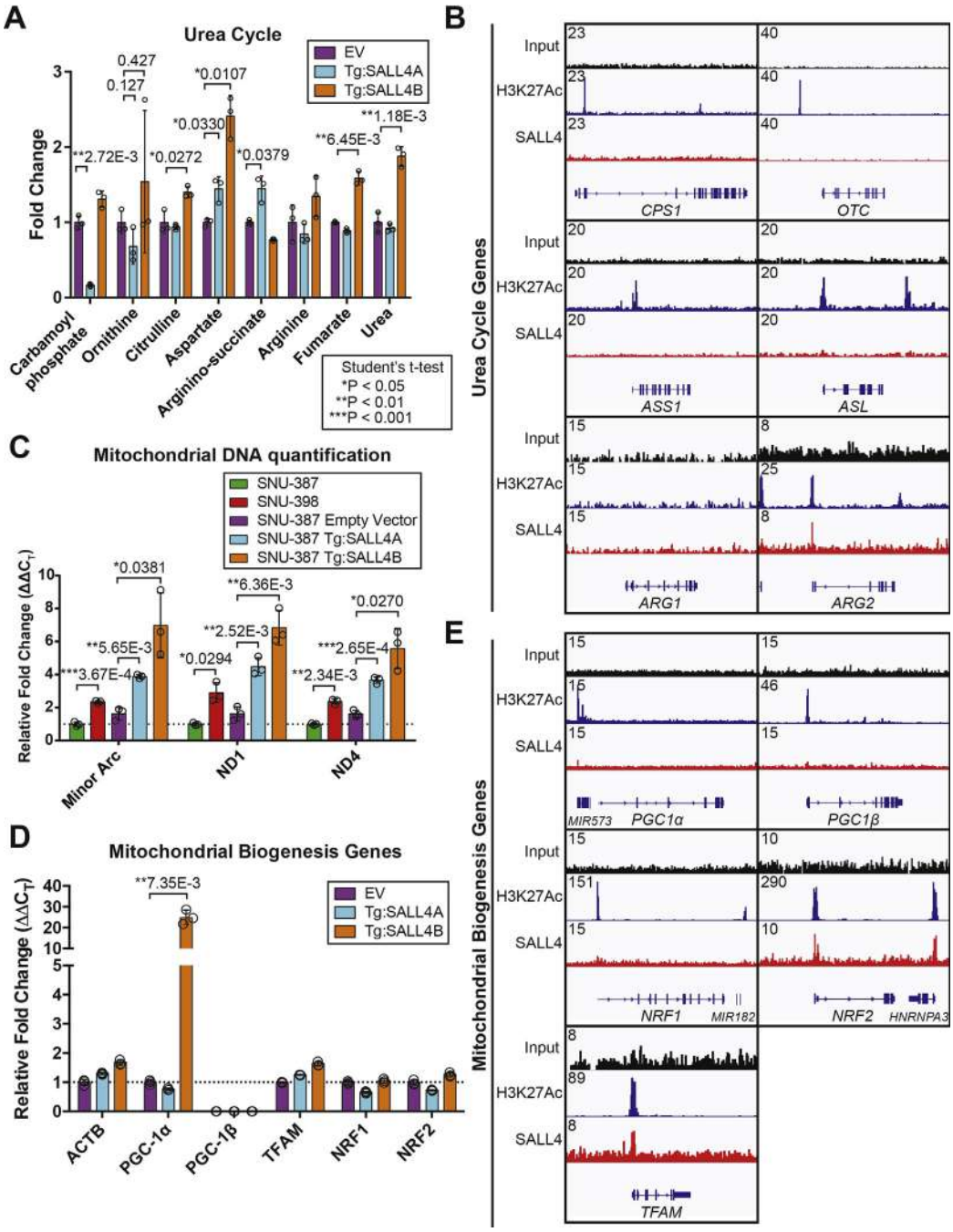

Supplementary Figure 7. SALL4 does not directly regulate the urea cycle and increases mtDNA copy number. (*A*) Fold change of urea cycle metabolites in the SALL4-expressing isogenic lines normalized to empty vector control (mean of 3 replicates ± SD). (*B*) Representative ChIP-seq input, H3K27ac, and SALL4 peaks for urea cycle genes. (*C*) mtDNA quantification with primers to the minor arc and *ND1* and *ND4* genes in *SALL4* endogenous and isogenic cell lines used in the screening, measured by qRT-PCR and normalized to *B2M* (mean of 3 replicates ± SD). (*D*) mRNA expression of mitochondrial biogenesis genes in the *SALL4*-expressing isogenic cell lines used in the screening, measured by qRT-PCR and normalized to *18S* ribosomal RNA (mean of 3 replicates ± SD). (*E*) Representative ChIP-seq input, H3K27ac, and SALL4 peaks for the mitochondrial biogenesis genes in (*D*).